Spring 2003

Development of a Force and Airspeed Data Acquisition System for the Embry-Riddle Aeronautical University 30x40 in. Subsonic Wind Tunnel

Toon Hong Foo
Embry-Riddle Aeronautical University - Daytona Beach

DEVELOPMENT OF A FORCE AND AIRSPEED DATA ACQUISITION SYSTEM FOR THE EMBRY-RIDDLE AERONAUTICAL UNIVERSITY 30×40 IN. SUBSONIC WIND TUNNEL

by

Toon Hong Foo

A Thesis Submitted to the
Graduate Studies Office
in Partial Fulfillment of the Requirements for the Degree of
Master of Science in Aerospace Engineering

Embry-Riddle Aeronautical University
Daytona Beach, Florida
Spring 2003

DATA ACQUISITION SYSTEM FOR WIND TUNNEL

by

Toon Hong Foo

This thesis was prepared under the direction of the candidate's thesis committee chairman, Prof. Charles Eastlake, Department of Aerospace Engineering, and has been approved by the members of his thesis committee. It was submitted to the Aerospace Engineering Department and was accepted in partial fulfillment of the requirements for the degree of Master of Science in Aerospace Engineering.

THESIS COMMITTEE

Charles N. Eastlake

Prof. Charles Eastlake
Chairman

Dr. Albert Helfrick
Member

Dr. Tej Gupta
Member

Eric V. K. Hill

Department Chair, Aerospace Engineering

1/4/03

Date

ACKNOWLEDGEMENTS

The author wishes to express thanks for the help and guidance of the thesis committee members in the completion of this thesis: Prof. Charles Eastlake, Dr. Albert Helfrick and Dr. Tej Gupta. Other staff of Aerospace Engineering Department, Mike Potash and Don Bouvier, contributed in making of the system hardware and provided advice in developing the system. The thesis would not be complete without their help and guidance.

The author would like to thank the support of the author's family and friends. The author's colleague in the wind tunnel lab, Ahmed El Nenaey, also contributed many useful suggestions in the troubleshooting of the system. Special appreciation goes to a good friend, Chai Yuet Yee, who has been providing spiritual support to the author for a long time.

ABSTRACT

Author: Toon Hong Foo

Title: Development of a Force and Airspeed Data Acquisition System for the Embry-Riddle Aeronautical University 30×40 inch Subsonic Wind Tunnel

Institution: Embry-Riddle Aeronautical University

Degree: Master of Science in Aerospace Engineering

Year: 2003

The very first objective of performing most experiments is collecting numerical data. Values can be read from instruments or gauges by eye and recorded by hand. However, in certain experiments the amount of data collected may become so large that a human alone can not observe and record the data fast enough. This is where a data acquisition system comes into play. A data acquisition system is a network of devices that collects data from intruments and outputs it to hard copies or storage devices. A data acquisition system can also control instruments to take the data at the exact moment and rate at which the user wishes. The system described in this thesis is capable of reading values from various instruments and reducing those data to yield aerodynamic loads, coefficients, temperatures and air velocities. Prior to 2000, a program wirtten in BASIC was used to control the data taking processes. This thesis will emphasise on the new data acquisition program written in the LabVIEW environment in 2000.

TABLE OF CONTENTS

ACKNOWLEDGEMENTS iv

ABSTRACT v

LIST OF TABLES x

LIST OF FIGURES xi

Chapter

1. BRIEF DESCRIPTION OF WIND TUNNEL, FORCE BALANCE AND OLD DATA ACQUISITION SYSTEM

   Instructional Subsonic Wind Tunnel 1

   Force Balance 3

   Old Data Acquisition System 4

2. BRIEF DESCRIPTION OF NEW DATA ACQUISITION SYSTEM, DATA ACQUISITION BOARD SPECIFICATIONS, COMPUTER PLATFORM AND PERIPHERAL EQUIPMENT

   New Data Acquisition System 5

   Board Specifications for PCI-6071E 7

   Input/Output 8

   Computer Platform 10

   LabVIEW® 11

   Pressure Transducer 11

   Temperature Sensor 13

3. DETAIL DESCRIPTION OF NEW DATA ACQUISITION SYSTEM 14

   Basic Subroutine: acq8chan.vi 15

First Sequence: Aerodynamic Tare 19

Second Sequence: Weight Tare 23

Third Sequence: Acquiring Data 25

Subroutine: MT.vi 27

Subroutine: velocity.vi 28

Fourth Sequence: Converting Loads into Coefficients 31

Sixth Sequence: Output 34

Calibration 36

4. OBSERVATIONS MADE DURING TESTING

Signal Amplification 40

Different Voltage Range of Transducer From Strain Gauges 42

Noise and Interference 43

5. RECOMMENDATIONS FOR THE FUTURE 47

Filter Solutions 47

Order of Running the Experiment 49

Print Out Format 51

Variable Force Balance Voltage Range 51

6. SAMPLE EXPERIMENTS 53

Exp 8 Drag of Bodies of Revolution

Introduction 53

Measured Data 54

Final Data 55

Conclusion 55

Exp 9A Forces Wing/fuselage/tail Model Buildup

Introduction 56

Measured Data 57

Final Data 59

Conclusion 61

Exp 11 Propeller Performance

Introduction 62

Measured Data 63

Final Data 64

Conclusion 67

REFERENCES 68

APPENDICES

A. Diagram Legend 69

B. Diagrams

Overall 71

Sequence 1 72

Sequence 2 74

Sequence 3 74

Sequence 4 78

Sequence 5 79

acq8chan.vi 82

MT.vi 83

velocity.vi 83

C. Block Diagrams

PCI-MIO-16E-1, PCI-MIO-16E-4 and NI PCI-6071E Block Diagram 84

P300D Pressure Transducer Block Diagram 85

D. Circuit Diagrams

Force Balance Pre-Amp System Circuit Diagram 86

Pressure Transducer Amplifier Circuit Diagram 87

LIST OF TABLES

Table 2.1 Actual Range and Measurement Precision, PCI-6071E 8

Table 2.2 Connector Blocks Differential Analog Input Table 10

Table 3.1 Channel Numbering System 17

Table 3.2 Calibration Factor of Force Balance Currently Used 37

Table 3.3 Pressure Transducer Calibration Factors 38

Table 5.1 Measured Drag Data 54

Table 5.2 Measured Data, Wing Alone 57

Table 5.3 Measured Data, Wing and Fuselage 57

Table 5.4 Measured Data, Wing, Fuselage and Tail 58

Table 5.5 Measured Data, Wing, Fuselage and Tail Incidence = -5^{o} 58

Table 5.6 Measured Data, Wing, Fuselage and Tail Incidence = -5^{o} and Landing Gear 59

Table 5.7 Measured Data, Static, Low β 63

Table 5.8 Measured Data, Static, High β 63

Table 5.9 Measured Data, Variable Velocity, High β 63

Table 5.10 Measured Data, Variable Velocity, Power off, High β 64

LIST OF FIGURES

Figure 1.1 Subsonic Instructional Wind Tunnel with Old HP Data Acquisition System 2

Figure 1.2 30×40 in. Subsonic Wind Tunnel Side Drawing 2

Figure 1.3 6-Channel Force Balance 3

Figure 2.1 Simplified Data Flow of Data Acquisition System 6

Figure 2.2 Validyne P300D Pressure Transducer 12

Figure 2.3 Pressure Transducers Mounting 13

Figure 3.1 WINDT2002 v2.0 Front Control Panel 15

Figure 3.2 Acq8chan.vi Front Control Panel 16

Figure 3.3 Acq8chan.vi Diagram 16

Figure 3.4 First Sequence Diagram 20

Figure 3.5 First Pop Up Dialogue Box 21

Figure 3.6 First Sub Frame of First Sequence 21

Figure 3.7 Second Pop Up Dialogue Box 22

Figure 3.8 Third Sub Frame of First Sequence 22

Figure 3.9 Choosing Old Aerodynamic Tare File 23

Figure 3.10 Third Pop Up Dialogue Box 24

Figure 3.11 Fourth Pop Up Dialogue Box 25

Figure 3.12 Fifth Pop Up Dialogue Box 25

Figure 3.13 Sixth Pop Up Dialogue Box 26

Figure 3.14 Vertical and Horizontal Moment Transfer 27

Figure 3.15 Moment Transfer 28

Figure 3.16 MT.vi Diagram 28

Figure 3.17 velocity.vi Diagram 29

Figure 3.18 Coefficient Calculation Diagram 32

Figure 3.19 Coefficient of Moment Calculation 33

Figure 3.20 Changing F_x into Drag 33

Figure 3.21 Result Printout with Loads Only 34

Figure 3.22 Result Printout with Drag and Coefficient of Drag only 35

Figure 3.23 Result Printout with Coefficients only 35

Figure 3.24 Result Printout with Loads and Coefficients 35

Figure 3.25 Sign Conventions Used in the Program 36

Figure 3.26 Force Balance Calibration Factor Table 37

Figure 3.27 Pressure Transducer Calibration Factor Table 39

Figure 4.1 Voltage Output from Drag Channel at 3400 RPM 45

Figure 4.2 Voltage Output from Drag Channel at 2500 RPM 45

Figure 4.3 Filter Test 48

Figure 5.1 Experiment 8 Set Up 54

Figure 5.2 Zero-lift Drag vs. Fineness Ratio 55

Figure 5.3 Experiment 9A Set Up 56

Figure 5.2 Coefficient of Lift vs. Angle of Attack 59

Figure 5.5 Coefficient of Drag vs. Angle of Attack 60

Figure 5.6 Coefficient of Pitching Moment vs. Angle of Attack 60

Figure 5.7 Experiment 11 Set Up 62

Figure 5.8 Static Thrust vs. RPM 64

Figure 5.9 Static Power Required vs. RPM 65

Figure 5.10 Thrust vs. V_o at Constant Power 65

Figure 5.11 RPM vs. V_o at with Power off 66

Figure 5.12 Drag vs. V_o at Power off 66

CHAPTER 1

Brief Description of Wind Tunnel, Force Balance and Old Data Acquisition System

1.1 Instructional Subsonic Wind Tunnel

There are three operational wind tunnels located in room LB176 of the Lehman Building at Embry-Riddle Aeronautical University. The wind tunnel most often used for both instruction and research is the 30×40 in. subsonic wind tunnel. It is an open circuit wind tunnel, powered by a 50 horsepower D.C. electric motor driving a 66-inch diameter fan with eight aluminum blades. The top speed of the tunnel is about 130 miles per hour without the intake screen and 115 miles per hour with the intake screen (to reduce turbulence level). The test section is 71 inches long, 40 inches wide and 30 inches high, and has a rectangular cross section. Construction material is primarily plywood. Air is supplied through an overhead door which opens to the outside of the building.

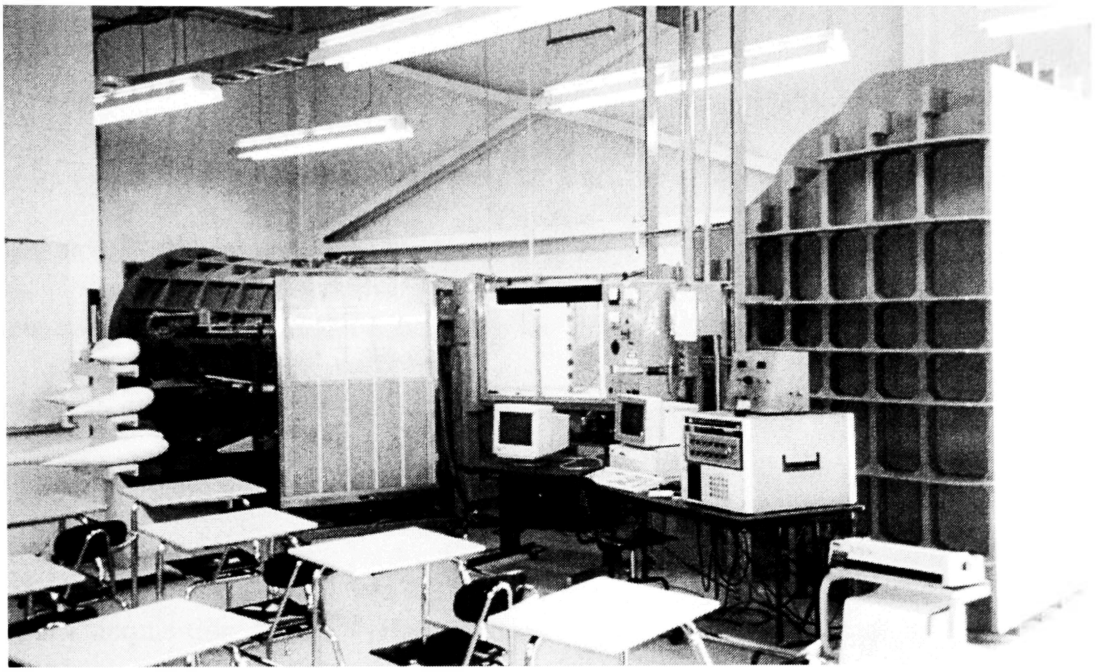

Figure 1.1 Subsonic Instructional Wind Tunnel with Old Hewlett Packard Data Acquisition System

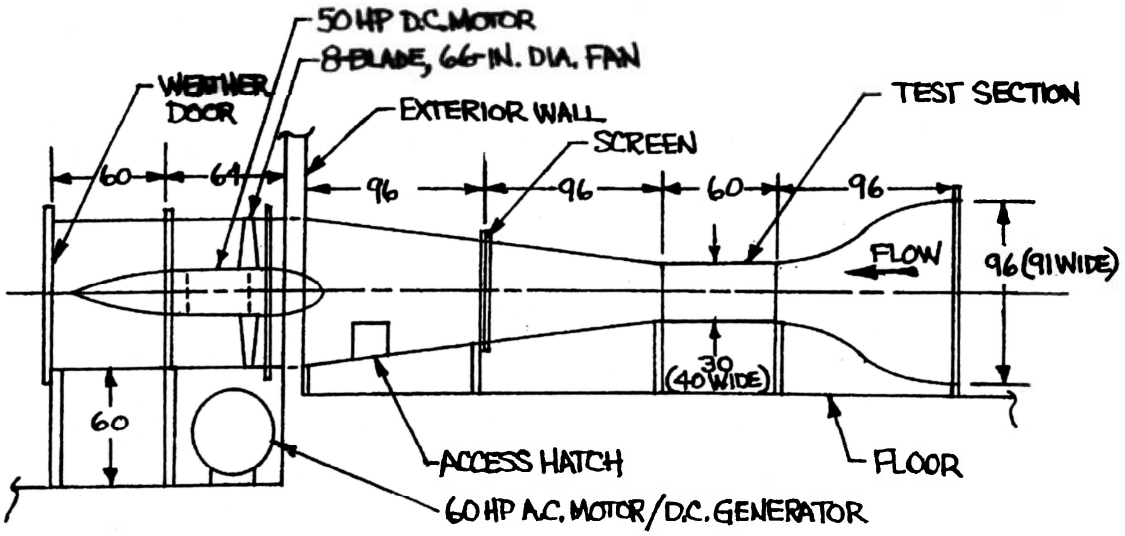

Figure 1.2 30×40 in. Subsonic Wind Tunnel Side Drawing, Dimension in inches (from Ref. 2)

1.2 Force Balance

A 6-channel pyramidal force balance built by AEROLAB of Laurel, Maryland is located below the test section. The balance is fitted with 6 load cells which give voltages in response to forces and moments applied along or about x, y, z axis system. The accuracy of the balance claimed by the manufacturer is ¼ of a percent of the full-scale capacities: lift = 100 lb, drag = 50 lb, side force = 50 lb, all moments = 100 in.lb. Currently, signals from each load cells are amplified by a factor of 1000 before output to the data acquisition board. The diagram of the amplifier circuit can be found in Appendix D.

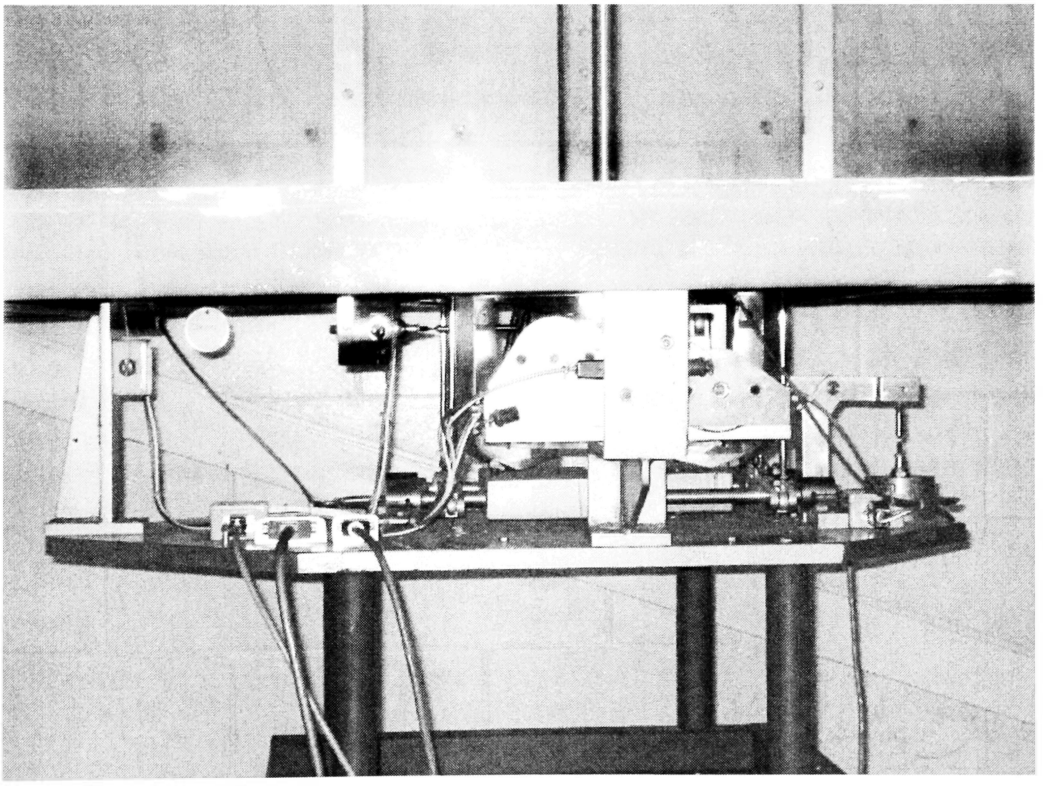

Figure 1.3 6-Channel Force Balance

1.3 Old Data Acquisition System

A Hewlett Packard 3497A data acquisition/control unit was used in conjunction with an IBM personal computer with Intel 80286 processor for almost 15 years. The program that controlled the data acquisition and performed computation, was written in BASIC language. It is written primarily by former Aerospace Engineering faculty member Mr. Glenn Greiner, who developed it from scratch to do precisely what was required to run this particular wind tunnel facility. This software worked well and was reliable as well as accurate. The HP 3497 is primarily an industrial process controller and was surprisingly trouble free throughout its long life in a lab which did not have temperature, humidity or dust control until the last 3 years of its use.

The decision to replace the system was based primarily on the emotional reaction of students to the system. All operating prompts, data input and data output were alphanumeric lines on a monochrome screen. Recent students simply did not identify with that format and found it uncomfortable to use. The decision was made in year 2000 to change over to a Windows-based system, which was predominantly a point and click operation. A National Instruments data acquisition board controlled by LabVIEW® was selected to accomplish this task.

CHAPTER 2

Brief Description of New Data Acquisition System, Data Acquisition Board Specifications, Computer Platform and Peripheral Equipments

2.1 New Data Acquisition System

The new data acquisition board was built by National Instruments. It is a PCI board installed inside a computer. It is a 12-bit board, which means that the smallest voltage it can measure is $(1/2)^{12}$ of the total range. Using the usual choice of ±10 V as the full scale output of the load cells, the board's resolution is ±4.88 millivolts with that range. The board is controlled by several VIs (virtual instruments) created in LabVIEW® environment. The following figure, Fig 2.1 represents the input and output of the system.

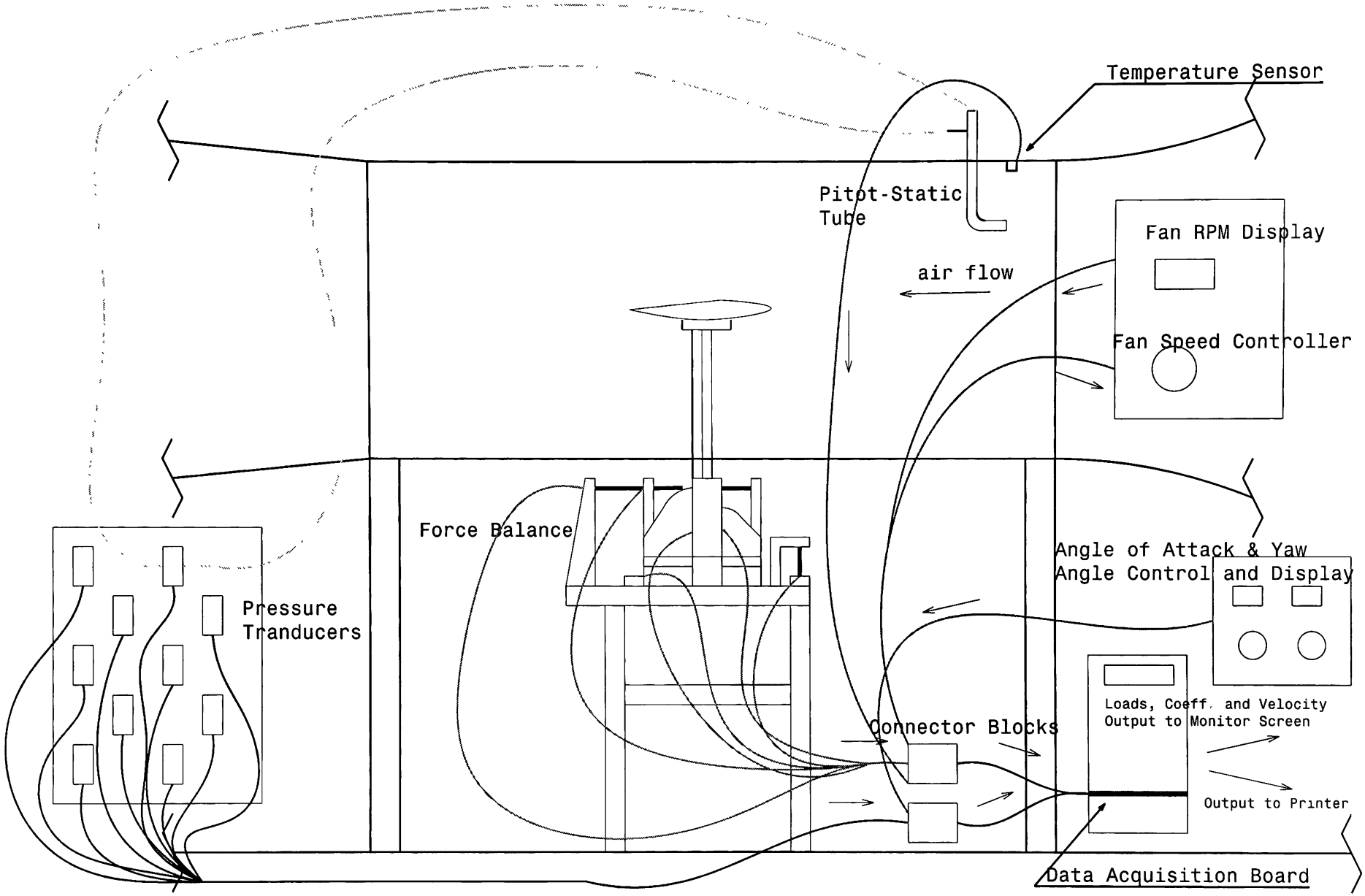

Figure 2.1 Simplified Data Flow of Data Acquisition System (not to scale)

2.2 Board Specifications for PCI-6071E

The data acquisition board is a National Instrument E Series board with PCI bus interface. It is a completely plug and play, timing, multifunction analog and digital input/output board for a PCI bus computer. Reference 4 provides detailed information about this data acquisition board. The card has 64 analog inputs, 2 analog outputs and 8 digital input/outputs available. It also has two 24-bit counter/timers for timing input/output. The E Series board is easily software-configurable and calibrated. [1]NI-DAQ® Driver software, register-level programming or application softwares such as LabVIEW®, ComponentWorks®, LabWindows/CVI® and VirtualBench® can be used with this board.

Data acquisition-related configuration such as analog input polarity and range and analog input mode can be performed through application level software such as NI-DAQ®, LabVIEW® and others. The PCI E Series boards have 3 different input modes, nonreferenced single-ended, referenced single-ended and differential input. The input mode and polarity used in described VIs (virtual instruments) here are differential and bipolar. By using differential input instead of single-ended input, it subtracts signals from two conductors instead a single conductor with respect to ground. This cancels the noise picked up by both conductors. The polarity and range can be configured on a per channel basis. Changing gain at the software-level can increase the overall flexibility by

[1] NI-DAQ®, LabVIEW®, ComponentWorks®, LabWindows/CVI® and VirtualBench® are registered trademarks of National Instruments.

matching the input signal ranges to those the analog-to-digital converter can accommodate. Different gains are suited for a wide variety of signal levels. The following table shows the overall input range and precision according to the input range configuration and gain used. A block diagram representing the board is available in Appendix C.

Table 2.1 Actual Range and Measurement Precision, PCI-6071E (from Ref. 4)

Range Configuration	Gain	Actual Input	Precision
0 to +10 V	1.0	0 to +9.99 V	2.44 mV
	2.0	0 to +4.99 V	1.22 mV
	5.0	0 to +1.99 V	488 μV
	10.0	0 to +0.999 V	244 μV
	20.0	0. to +499 mV	122 μV
	50.0	0 to +199 mV	48.8 μV
	100.0	0 to +99.9 mV	24.4 μV
-5 to +5 V	0.5	-9.99 to +9.99 V	4.88 mV
	1.0	-4.99 to +4.99 V	2.44 mV
	2.0	-2.49 to +2.49 V	1.22 mV
	5.0	-0.999 to +0.999V	488 μV
	10.0	-499 to +499 mV	244 μV
	20.0	-249 to +249 mV	122 μV
	50.0	-99.9 to +99.9 mV	48 μV
	100.0	-49.9 to +49.9 mV	24 μV

2.3 Input/Output

Six analog inputs are used for the force balance. Ten analog inputs are used for the pressure transducers. One analog input is used for the temperature sensor. In addition, there are other installed input/output not used in VIs described in this paper.

There are two analog inputs to indicate angle of attack and yaw angle. Two potentiometers each control the angle of attack and yaw angle by changing the input voltages of the servo motors located within the force balance. An amplifier circuit outputs the voltages to the board. There is one analog input for the fan tachometer and one analog output for controlling the fan speed. There is a frequency to voltage converter used for outputting a corresponding voltage to the board for measuring the fan RPM. The control over the fan speed is achieved by pulse width modulation. By increasing the duty cycle of the pulses, the D.C. generator that powers the fan output more power and therefore increases the fan speed. This fan speed control is not currently being used but probably will be used in the future.

All inputs/output wirings use shielded twisted pairs to minimize noise pick up. The twisted pairs are hooked up to two National Instruments SCB-68 connector blocks. The connector blocks output to a shielded National Instruments SH1006868 cable through two 68-pin connector. The other end of the cable has a 100-pin connector and is connected to the data acquisition board. The following table illustrates the corresponding functions and channels in the connector blocks. The detailed description of the SCB-68 connector block can be found in reference 5.

Table 2.2 Connector Blocks Differential Analog Input Table

Connector block	Differential analog channels	Function	Channel in LabVIEW®
1	0 and 8	Temperature	0
	1 and 9	Force Balance Lift	1
	2 and 10	Force Balance Drag	2
	3 and 11	Force Balance Pitch	3
	4 and 12	Force Balance Roll	4
	5 and 13	Force Balance Yaw	5
	6 and 14	Force Balance Side Force	6
	7 and 15	Fan RPM	7
2	16 and 24	Pressure Transducer 1	16
	17 and 25	Pressure Transducer 2	17
	18 and 26	Pressure Transducer 3	18
	19 and 27	Pressure Transducer 4	19
	20 and 28	Pressure Transducer 5	20
	21 and 29	Pressure Transducer 6	21
	22 and 30	Pressure Transducer 7	22
	23 and 31	Pressure Transducer 8	23
	32 and 40	Pressure Transducer 9	24
	33 and 41	Pressure Transducer 10	25
	35 and 43	Angle of Attack	26
	36 and 44	Yaw Angle	27

2.4 Computer Platform

The computer used now is a Dell Dimension XPS P100 personal computer with Pentium® 100 MHz processor. The operating system is Windows 95. It is a stand alone system which is dedicated to the wind tunnel data acquisition. It is not connected to the campus network. A Hewlett Packard DeskJet 1100 laser jet printer is connected to it for hardcopy output and it can make multiple copies for handout to class members.

2.5 LabVIEW®

LabVIEW® is an application software developed by National Instruments for data acquisition. It features interactive graphics, a state-of-the-art user interface, and a powerful graphical programming language. LabVIEW® has a Data Acquisition VI Library with a series of VIs for using LabVIEW® with National Instruments boards.

LabVIEW® is an industry standard in data acquisition software. One of the reasons for using the LabVIEW® is because it has a point and click graphical user interface instead of the DOS prompt input lines in the old BASIC program. This would allow the program to be very user-friendly to those who have grown up in Windows era (instead of DOS), especially the younger students.

2.6 Pressure Transducer

Ten Validyne P300D differential pressure transducers are available for use in conjunction with the system to measure pressure. A differential pressure transducer has a sensing diaphragm inside a symmetric cavity in which both sides of the diaphragm are connected to places where pressure needs to be known. Both ends of the default transducer are hooked up to the Pitot–static probe in the test section, to find out the difference between total and static pressure in the test section. The difference is also called dynamic pressure. The transducer range of measurement is ± 0.8 pounds per

square inch. The block diagram of the pressure transducer can be found in Appendix C. The accuracy claimed by the manufacturer is ±0.5% of full scale.

In the beginning of Fall semester 2002, an amplifier with a amplification factor of 100 was added to pressure transducer number 2, the default transducer. The amplifier's circuit diagram is illustrated in Appendix D. The detailed information about the P300D pressure transducer can be found in reference 6.

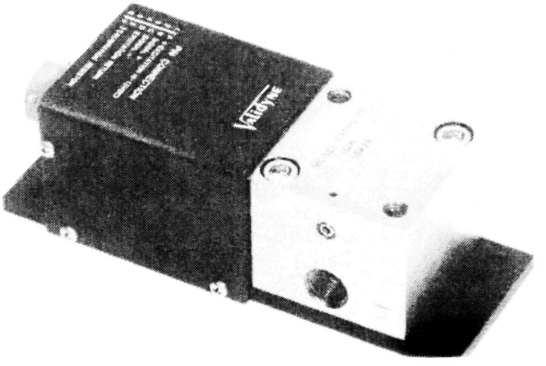

Figure 2.2 Validyne P300D Pressure Transducer (from Ref. 6)

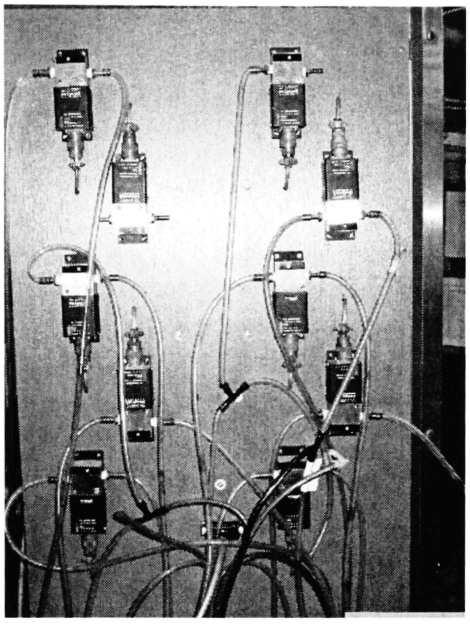

Figure 2.3 Pressure Transducer Mounting

2.7 Temperature Sensor

A National Semiconductor LM34 precision Fahrenheit temperature sensor is located at the top of the test section to provide temperature reading. It is an integrated circuit designed to measure temperatures from -50° to 300° F. For every degree Fahrenheit, the voltage output changes by 10 mV. The signal is amplified before outputting to the data acquisition board. It is hooked up to the system to allow temperature to be taken simultaneously with the dynamic pressure in order to calculate test section air velocity.

CHAPTER 3

Detailed Description of New Data Acquisition System

The entire main program is divided into sequences, in which each performs a number of tasks and then passes on the numbers into next sequence To ensure the diagram is easy to see and not overly tangled with lines representing flows of data, some often-repeated tasks are organized into subroutines called sub VIs (Virtual Instruments) in LabVIEW® terminology denoted by special symbols Since the subroutines are saved in " vi" files as the main program, they can be run separately (without the main program) for diagnostics The main program is named WINDT200X, the last characters represent the year in which the program weas first used In some years, more than one version of the main program was created due to upgrades and special version for a particular task In that case a version digit, X 0 will follow the WINDT200X name For instance, the example used in this paper is WINDT2002 v2 0, which is scheduled to be used in Fall 2002

What the user sees when the program is started is a front control panel in which the user can input numbers and the results are displayed For upgrading and diagnostics, the front panel can easily be switched to a diagram in the form of flowchart

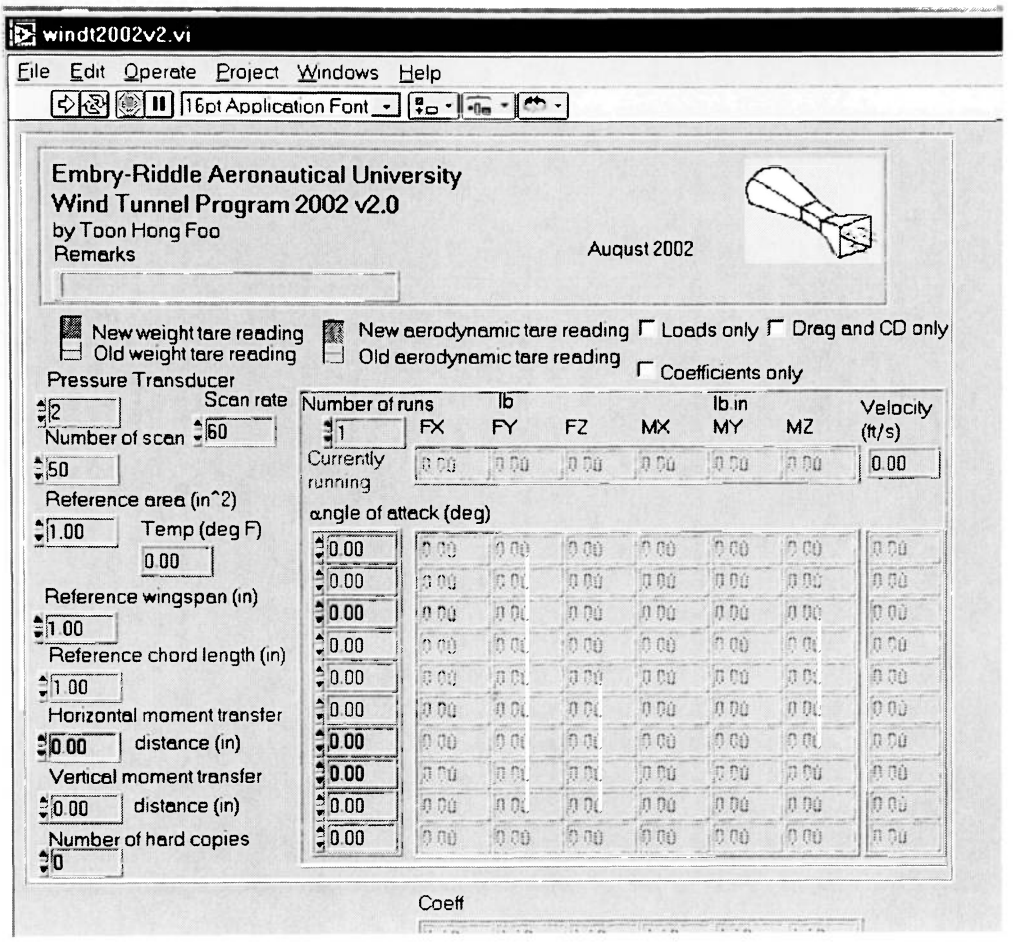

Figure 3.1 WINDT2002 v2.0 Front Control Panel

Subroutines used are acq8chan.vi, velocity.vi, replacecolumn.vi and MT.vi. Their purposes are described below.

3.1 Acq8chan.vi

Acq8chan is the basic building block of the main program. It is called upon many times. The diagram of acq8chan.vi is shown next.

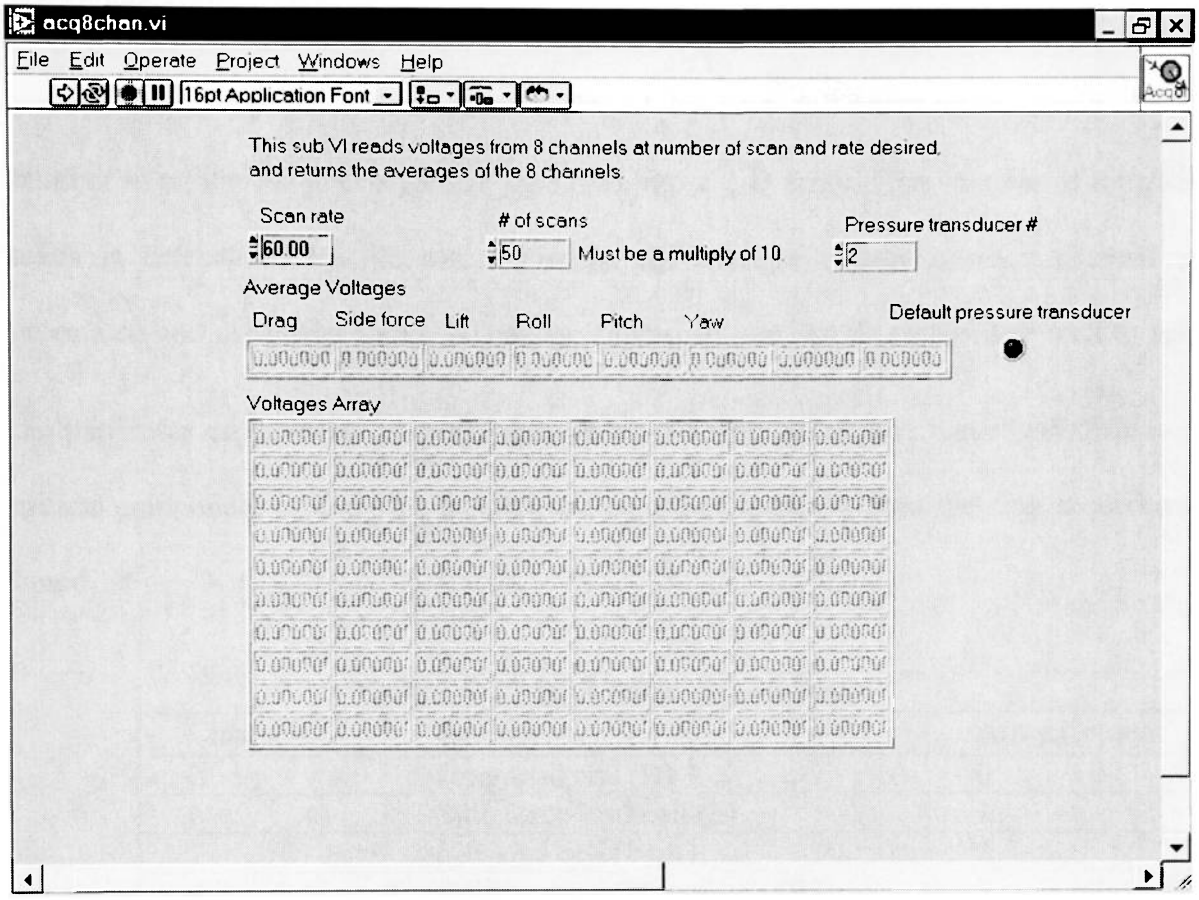

Figure 3.2 Acq8chan.vi Front Control Panel

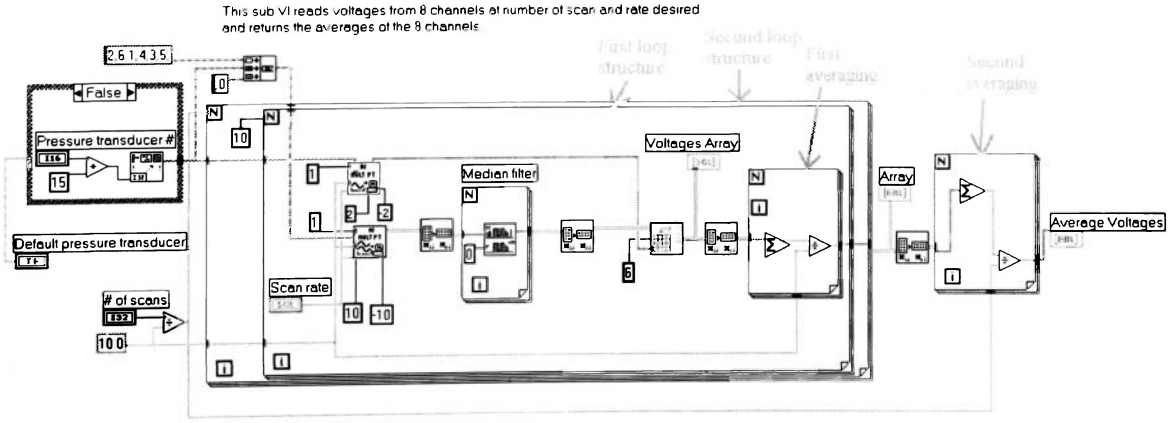

Figure 3.3 Acq8chan.vi Diagram

When used, this subroutine will read the voltages from all six channels of the force balance, a pressure transducer indicated by user and temperature sensor for a number of times and then organizes that data into a 2-D array. The number of samples taken is determined by the user. Finally, the average voltage of each channel is calculated and organized into a 1-D array. The scan rate can be changed as well to suit the particular experiment. A preprogrammed VI called AI acquire waveform,  is a critical component of that VI. It reads analog inputs channels from the data acquisition board.

Table 3.1 Channel Numbering System

Channel	Source	Array Column
2	Drag load cell (D)	0
6	Side force load cell (S)	1
1	Lift load cell (L)	2
4	Rolling moment load cell (R)	3
3	Pitching moment load cell (P)	4
5	Yawing moment load cell (Y)	5
16 to 25	Pressure transducers 1 to 10	6
0	Temperature sensor	7

The channels are scanned in the order shown by the above table. The AI acquire waveform  is used twice. The reason is that the pressure transducer voltage is taken a second time with a different scale. A detail description of why it is done is explained in section 4.2.

The true or false case structure on the upper left corner lights up a "light bulb" on the front panel when the default transducer is used. A value fifteen is added to the pressure transducer number to yield channel number for that particular pressure

transducer. Transducer number 1 uses channel 16, transducer number 2 uses channel 17 and so on.

Another function median filter  is seen here. It can be turned on if the data fluctuates too much.

The next step is the replacecolumn.vi  . It replaces the column with pressure transducer voltages taken first time with the ones taken second time at different scale. The pressure transducer have a different output range from the force balance. The first AI acquire waveform  will read all the channels at a scale best for force balance and the second will read all the channels at a scale best for pressure transducer.

The number of scans is in multiples of ten (10, 20, 30 .....). Suppose for example that 50 scans is chosen by the user, the subroutine will first read the voltage from a channel and then go to the next one. After all the channels have been read, the process will be repeated 10 times. This is represented by the "First loop structure" indicated in Figure 3.3. After that, the values will be averaged, as shown by the "First averaging" for loop with summation and division function in it. Then, the above process will be repeated 5 (50 divided by 10) times, represented by the outer "big" for loop as indicated as "Second loop structure" in Figure 3.3. The final values are averaged again in the "Second averaging" for loop with summation and division function in it. The averaging of multiple data points is done to minimize influence of fluctuations in the data being read.

Several transpose array functions  are seen before and after each calculation. The reason is that the array is arranged such that each column represents a channel, but the calculations done to array requires that the data from each channel be in rows.

3.2 Aerodynamic Tare

The zeroth sequence (or frame) reads the angles of attack for the set of runs from the front panel and put them into an array "Alpha". The sequence number is located at the top of the frame. The reason why the first sequence is named "zeroth" is that sequence structure in LabVIEW® starts with zero by default. The same goes with array and loop structure.

The first sequence basically deals with aerodynamic tare. When a model is tested in a wind tunnel, the only forces needed are the aerodynamic forces acting on the model. Any forces or moments acting on the supporting post for the model should be subtracted away. The loads acting on the support are called aerodynamic tare. Drag is the force in most obvious, and drag also influences pitch moment. But aerodynamic tare corrections are made to all the six balance channels.

The true or false box  in the middle of first sequence gives the user choice of using an existing aerodynamic tare file stored on the hard drive or a floppy disk, or measuring a new aerodynamic tare from scratch.

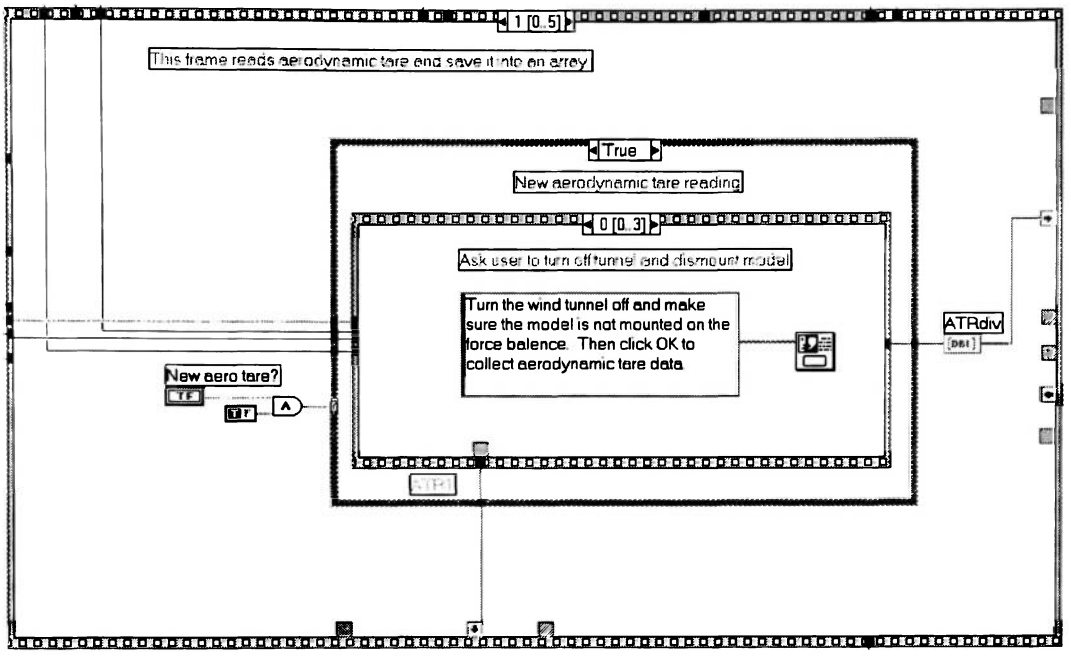

Figure 3.4 First Sequence Diagram

There is a Boolean button on the WINDT2002 front panel to allow the user to choose. The false side of the box is for the old aerodynamic tare, and the true side of the box is for the new aerodynamic tare.

If new aerodynamic tare is chosen, a dialog box will pop up to inform the user to turn off the tunnel and dismount the model.

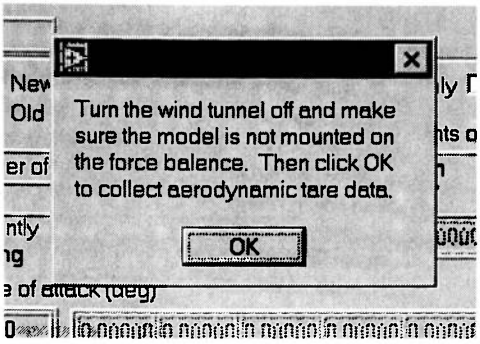

Figure 3.5 First Pop Up Dialog Box

After the user clicks the "OK" button on the dialog box, the acq8chan.vi subroutine is initiated and takes the voltages from all the channels of the force balance as shown in the next sub frame.

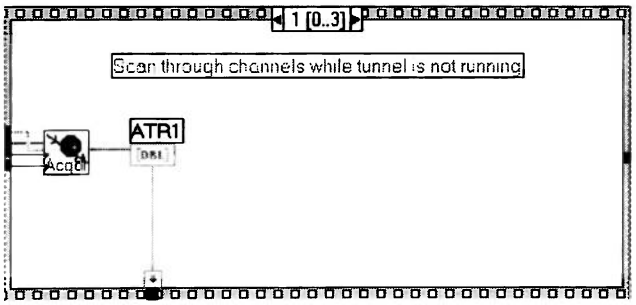

Figure 3.6 First Sub Frame of First Sequence

The data is put into an array called "ATR1" Then, another dialog box will pop up and ask the user to turn the tunnel on.

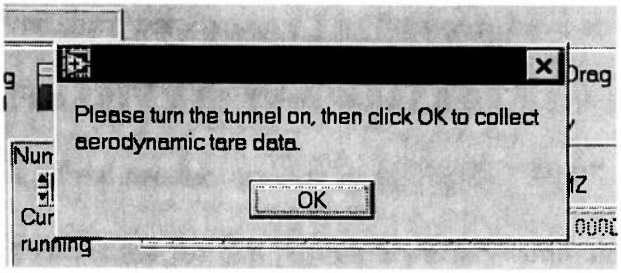

Figure 3.7 Second Pop Up Dialog Box

After the user clicked "OK", acq8chan.vi will be called upon again to take another set of voltages while the tunnel is running, as shown in the third sub frame.

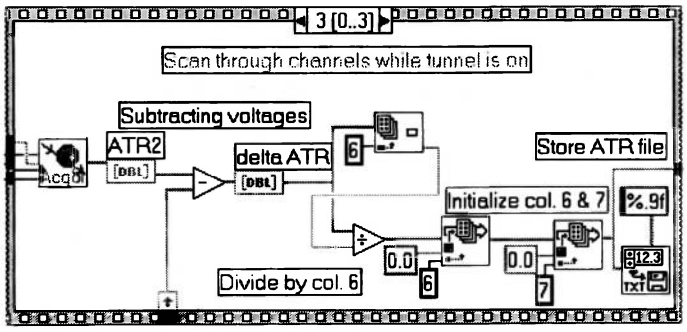

Figure 3.8 Third Sub Frame of First Sequence

The data goes to an array called "ATR2". Then the difference between the array "ATR1" and "ATR2" is taken. After that, the entire difference array called "delta ATR" is divided by the value from pressure transducer, taken out of the array itself by using the function index array. The number "6" that goes into the index array function box  means column six of the array, which is for pressure transducer voltage.

Then, column six (pressure transducer) and seven (temperature sensor) is reset to zero. All arrays in this program containing voltage data have eight columns ranges from

zero to seven. However since aerodynamic tare files only have six elements, so in order to make the intermediate array looks clear, values that are not used subsequently are replaced with zero. The final product will be named array "ATR". Finally, the user will be prompted to input a file name for that particular aerodynamic tare file, to be stored on either the hard drive or a floppy disk. The file is in .dat format.

If the user chooses to use an existing aerodynamic tare file, the user will be prompted to choose the file from the hard drive or a floppy disk.

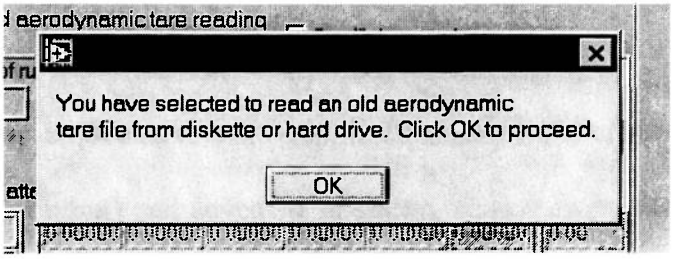

Figure 3.9 Choosing Old Aerodynamic Tare File

3.3 Weight Tare

The second sequence deals with weight tare. Since aerodynamic forces on the model are the only forces of interest to the user, the weight of the model must be taken out as well. The process is done in manner similar to that of the previous sequence.

Again, a true or false box is used. True means new weight tare, false means old weight tare. If the user chooses new weight tare, a dialog box will appear asking the user to turn the tunnel off and mount the model.

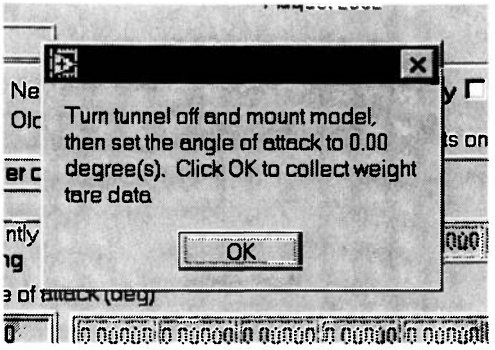

Figure 3.10 Third Pop Up Dialog Box

After that, the acq8chan.vi will be initiated and read the voltages. The column six (pressure transducer output) and seven (temperature sensor output) is initialized to zero. Only values from the first six columns from the array "WTR" are used subsequently, anything which is not used is replaced with zero to show clarity. The above process will be repeated several times, once for each angle of attack. The number of times it will be repeated is controlled by the "number of runs" input box on the front panel. The final product is compiled into the array "WTR". The user will be prompted for a file name under which to save the weight tare file.

If the user chooses an old weight tare, an existing file will be opened from hard drive or floppy disk after the user responds by giving the file name to be used. As in aerodynamic tare, the file format for weight tare is .dat.

3.4 Acquiring Data

The third sequence is the most complicated one. The first process is a pop up dialog box telling the user to turn on the tunnel.

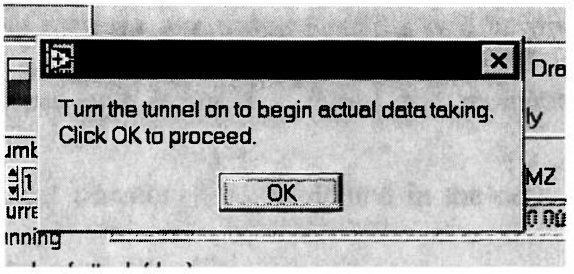

Figure 3.11 Fourth Pop Up Dialog Box

After that, another dialog box will appear to tell the user to set the first angle of attack. The angles of attack have been listed in the table on the front panel by the user and this subroutine reads them one at a time beginning at the top of the table.

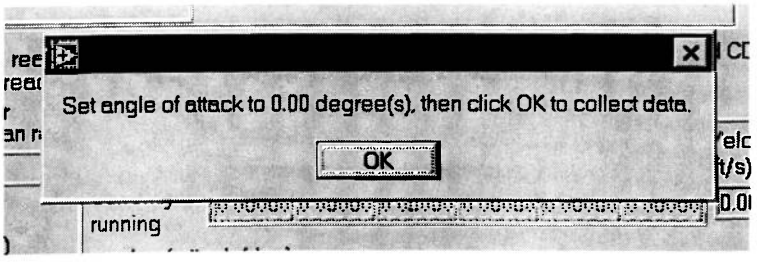

Figure 3.12 Fifth Pop Up Dialog Box

Then, the next sub sequence will call upon the acq8chan.vi to gather the voltages. The result will be stored in an array called "Volt". By subtracting the array "ATR1",

which is the initial reading, this gives the active wind tunnel on reading. Then, that array will subtract two arrays. The first to be subtracted is the result of array "ATR" multiplied with the column six (voltage from pressure transducer) which is the aerodynamic tare. The next to be subtracted is array "WTR" which is the weight tare.

After the tare subtractions, the voltage results will be divided by the calibration factors to yield the forces and moments. Then, the moments will go through the subroutine MT.vi (moment transfer)  , explained in the next section. The corrected results will be put into the array "Load".

The above process will be repeated for the number of runs specified. The forces and moments will be shown across the top of the data box on the front panel after each run. A dialog box will pop up and ask whether the user accepts the values or not. If the user feels something was wrong with the data and chooses not to accept it, it will be repeated and presents a new set of forces and moments.

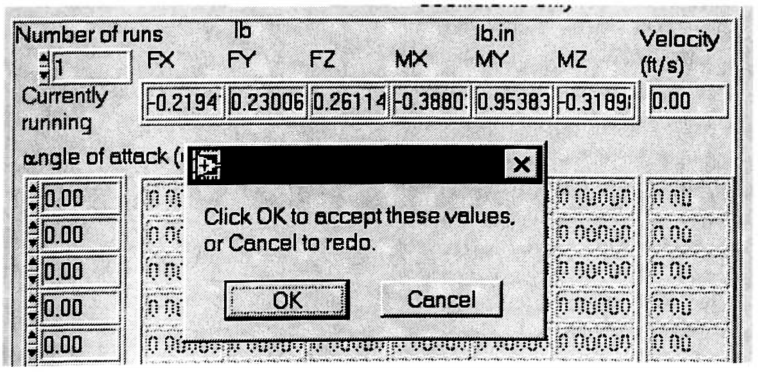

Figure 3.13 Sixth Pop Up Dialog Box

3.5 Moment Transfer

The calibration is done with loads applied to the reference point of the force balance, which is the point at which the centerline of the supporting post intersects the model mounting plate. However, it is not often possible to have that point coincide with the center of gravity (C.G.) of the model. In order to find out the equivalent moments at the C.G., the moments measured at the reference point must go through a moment transfer correction. Needed inputs for the transfer are the vertical and horizontal distances between the reference point and C.G, namely vertical moment transfer (VMT) and horizontal moment transfer (HMT).

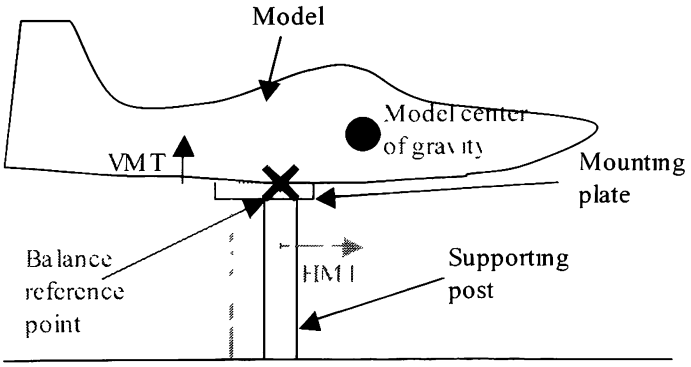

Figure 3.14 Vertical and Horizontal Moment Transfer

$$M_{x_{corrected}} = M_x - VMT \times F_y$$
$$M_{y_{corrected}} = M_y - HMT \times F_z + VMT \times F_x$$
$$M_{z_{corrected}} = M_z - HMT \times F_y$$

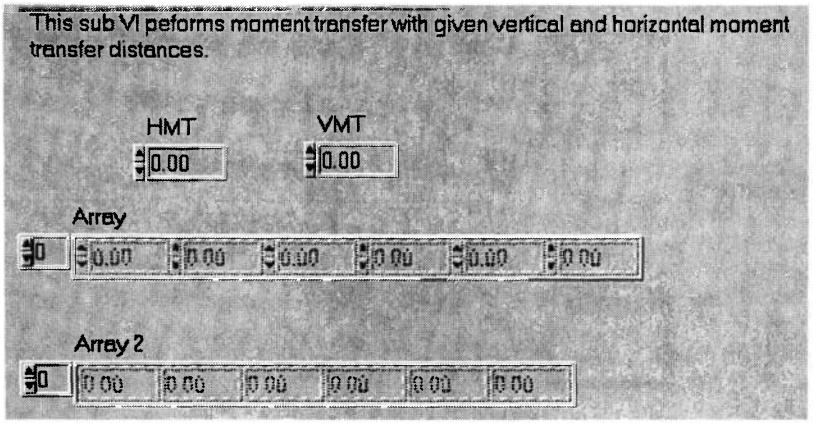

Figure 3.15 Moment Transfer

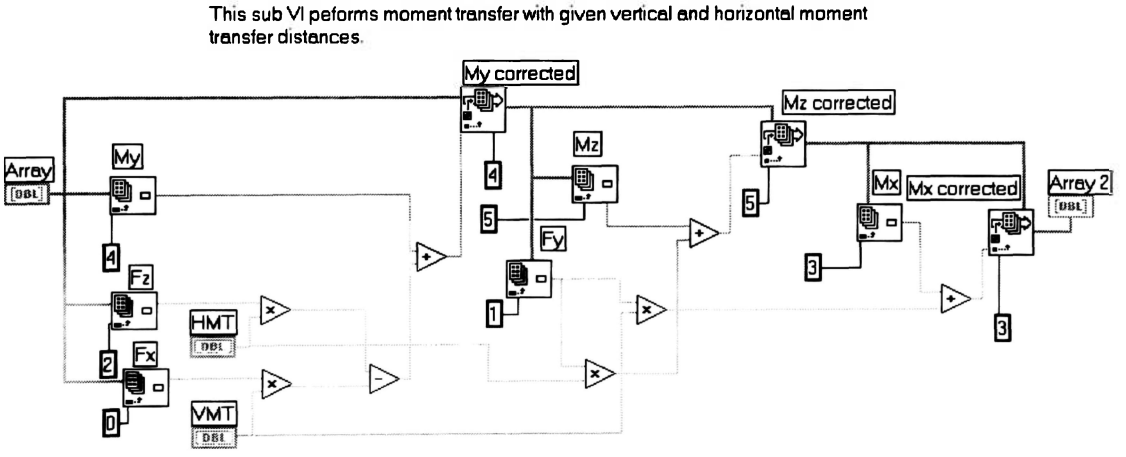

Figure 3.16 MT.vi Diagram

3.6 Velocity

A subroutine called velocity.vi is used to calculate air velocity in the wind tunnel using the temperature reading from the temperature sensor and the difference between total and static pressures from the pressure transducer.

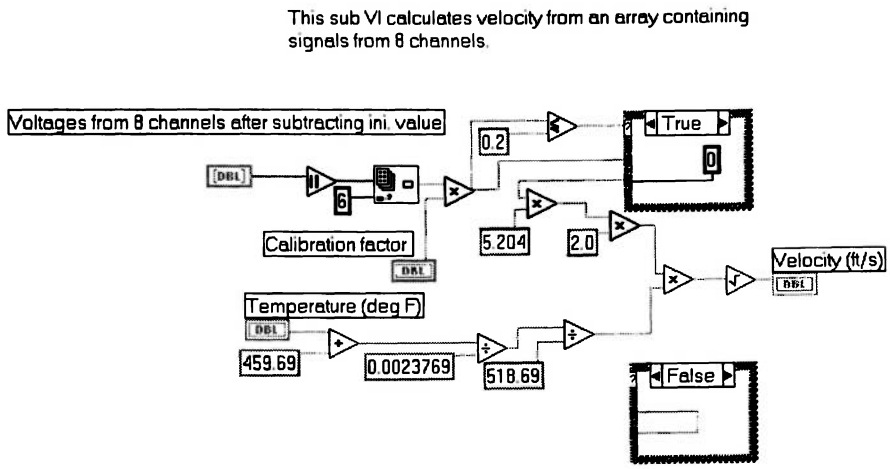

Figure 3.17 velocity.vi Diagram

The voltage from one of the channels between channel 16 and 25, after subtracting the initial value to yield active wind tunnel on reading, is multiplied by the calibration factor. This gives the pressure difference in inches of water (in. H_2O). The difference is also known as dynamic pressure (q).

If the pressure difference is less than 0.2 inches of water, meaning that the velocity is very low, it is simply replaced by zero in order to yield zero velocity. The reason behind this is that the background small drift in the electrical system is sometimes sufficient to produce a low velocity output voltage even when the actual velocity in the test section is zero (because the tunnel is not running). A small amount of calculated velocity is sufficient to cause small aerodynamic tare corrections to be incorrectly incorporated into the wind-off data. Thus, removing the small velocity improves the accuracy of wind off data and making sure that all balance channels read essentially zero before beginning an experiment.

The pressure difference is then multiplied by 5.204, which converts inch of water into pound per square foot (psf) for easier calculation. Bernoulli's principle is then applied to find out the velocity.

P_{static} = static pressure (psf)
P_{total} = total pressure (psf)
V = air velocity (ft/s)
ρ = air density (slug/ft^3)
T = air temperature (degree Rankine)

$$P_{total} = P_{static} + \frac{1}{2}\rho V^2$$

$$\frac{1}{2}\rho V^2 = P_{total} - P_{static}$$

$$V = \sqrt{\frac{2(P_{total} - P_{static})}{\rho}}$$

The air density is inversely proportional to temperature. So, if provided with standard sea level (SSL) density and temperature, the density at a known temperature can be found, assuming that atmospheric pressure does not vary significantly from the standard sea level value (this wind tunnel is very close to sea level, at 39 ft).

$$\rho T = \rho_{SSL} T_{SSL}$$

$$\rho = \rho_{SSL} T_{SSL} / T$$

The SSL temperature is 518° Rankine, while SSL air density is 2.3769×10^{-3} slugs/ft^3. The final velocity is given in ft/s.

3.7 Converting Loads into Coefficients

In aerodynamics, it is usually most convenient to express aerodynamic data as not the absolute load, but the dimensionless coefficient form of that load. The three forces and three moments obtained in the third sequence are converted into six coefficients in the fourth sequence.

C_{Fx} = coefficient of force along positive x-axis
F_x = force in positive x-axis (lb)
V = air velocity (ft/s)
ρ = air density (slugs/ft^3)
C_{Mx} = coefficient of moment about positive x-axis
M_x = moment about positive x-axis (in.lb)
S_{ref} = reference wing area (ft^2)
b_{ref} = reference wing span (ft)
c = mean aerodynamic chord length (ft)

$$C_{F_x} = \frac{2F_x}{\rho V^2 S_{ref}}$$

$$C_{F_y} = \frac{2F_y}{\rho V^2 S_{ref}}$$

$$C_{F_z} = \frac{2F_z}{\rho V^2 S_{ref}}$$

$$C_{M_x} = \frac{2M_x}{\rho V^2 b_{ref} S_{ref}}$$

$$C_{M_y} = \frac{2M_y}{\rho V^2 \bar{c} S_{ref}}$$

$$C_{M_z} = \frac{2M_z}{\rho V^2 b_{ref} S_{ref}}$$

The loop box on the left basically divide the loads in array "Load" by the dynamic pressure, or $1/2\rho V^2$ and reference area (S_{ref}).

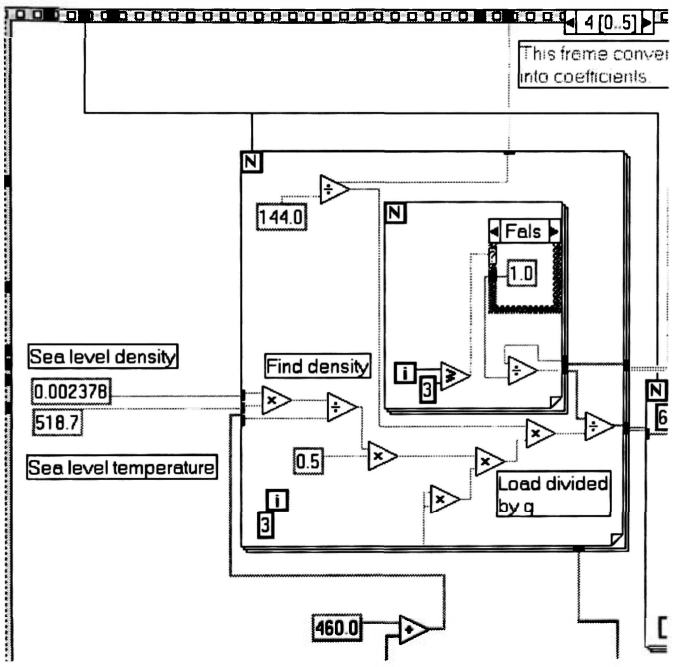

Figure 3.18 Coefficient Calculation Diagram

The density is found in the same manner as described in velocity.vi. The small loop box within the first box on the left basically passes the moments (column three and above) into another loop box which basically divides by an extra term reference chord length (c) or reference wingspan (b_{ref}) as defined in the equations above.

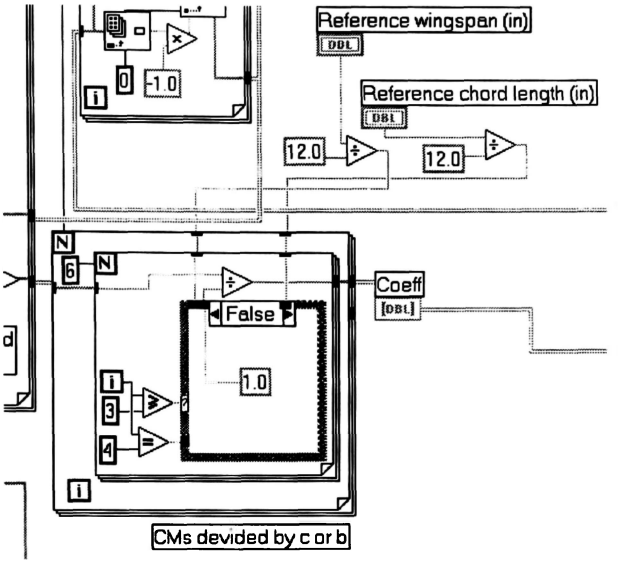

Figure 3.19 Coefficient of Moment Calculation Diagram

S_{ref}, b_{ref} and c are input from the front panel, and if the user does not wish to use them, the default value is one. The final calculated products are arranged into an array called "Coeff".

The last loop box on the right basically converts thrust (column zero) to drag and by multiplying it by minus one. The resulted array is named "Load, final" for output and coefficient calculation.

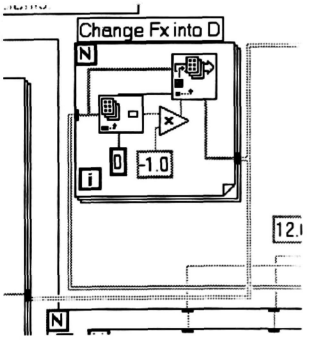

Figure 3.20 Changing F_x into Drag

3.6 Output

The user has several options for output. The results will be printed and saved into the hard drive or a floppy disk. The number of copies of printout is controlled by a digital input on the front panel. If the user chooses not to print any result, a number zero shall be put there. The user can choose all loads and coefficients, only loads, only coefficients or only drag and coefficient of drag to be printed and saved. The choice is selected by several check boxes ☐ on the front panel. On the diagram, that selection process is done by a series of true or false boxes within each other.

Angles of attack, velocities and temperatures are stored in separate arrays (Alpha, Velo and Temp) until this final output process. A compile function,  , will join the 3 arrays together with arrays "Load" and "Coeff" to form one big array (depending on choice). Then, row and column headers are added to form a complete table. Extra information like program version number, date and time is printed on top of the print out.

Embry-Riddle Aeronautical University 2/3/03 3:07 PM
Wind Tunnel Data Acquisition Summary
WINDT2002 v2.0

	AOA (deg)	D (lb)	FY(lb)	L (lb)	MX	MY	MZ	V	Temp
Run 1	0.00	-0.01	0.02	0.05	-0.02	0.55	-0.93	62.87	69.89
Run 2	0.00	0.00	0.01	0.05	0.06	0.47	-0.94	63.99	69.90
Run 3	0.00	-0.03	-0.02	0.07	-0.08	0.39	-0.96	63.47	69.91
Run 4	0.00	-0.08	0.05	0.09	-0.00	0.17	-0.93	63.24	70.18
Run 5	0.00	-0.02	0.00	0.02	-0.18	0.52	-0.95	63.61	70.23
Run 6	0.00	0.00	0.00	0.00	0.00	0.00	0.00	0.00	0.00
Run 7	0.00	0.00	0.00	0.00	0.00	0.00	0.00	0.00	0.00
Run 8	0.00	0.00	0.00	0.00	0.00	0.00	0.00	0.00	0.00
Run 9	0.00	0.00	0.00	0.00	0.00	0.00	0.00	0.00	0.00
Run 10	0.00	0.00	0.00	0.00	0.00	0.00	0.00	0.00	0.00

Figure 3.21 Result Printout with Loads Only

Embry-Riddle Aeronautical University 2/3/03 2:55 PM
Wind Tunnel Data Acquisition Summary
WINDT2002 v2.0

	AOA (deg)	D (lb)	CD	V (ft/s)
Run 1	0.00	0.01	0.32	64.09
Run 2	0.00	-0.02	-0.56	66.33
Run 3	0.00	0.01	0.35	66.42
Run 4	0.00	-0.05	-1.24	67.07
Run 5	0.00	-0.01	-0.29	67.59
Run 6	0.00	0.00	0.00	0.00
Run 7	0.00	0.00	0.00	0.00
Run 8	0.00	0.00	0.00	0.00
Run 9	0.00	0.00	0.00	0.00
Run 10	0.00	0.00	0.00	0.00

Figure 3.22 Result Printout with Drag and Coefficient of Drag only

Embry-Riddle Aeronautical University 2/3/03 2:49 PM
Wind Tunnel Data Acquisition Summary
WINDT2002 v2.0

	AOA (deg)	CD	CFY	CL	CMX	CMY	CMZ	V (ft/s)	Temp
Run 1	0.00	-0.32	0.12	1.34	-3.55	17.44	-29.01	62.98	70.39
Run 2	0.00	-0.11	1.04	0.71	0.51	10.29	-26.79	65.97	70.35
Run 3	0.00	0.60	1.04	1.50	-2.62	12.59	-26.98	65.87	70.28
Run 4	0.00	-1.84	1.20	1.54	-3.67	0.83	-27.08	65.75	70.15
Run 5	0.00	-0.52	1.39	-0.11	-3.23	18.36	-26.42	66.12	70.16
Run 6	0.00	0.00	0.00	0.00	0.00	0.00	0.00	0.00	0.00
Run 7	0.00	0.00	0 00	0.00	0.00	0.00	0.00	0.00	0.00
Run 8	0.00	0.00	0.00	0.00	0.00	0.00	0.00	0.00	0.00
Run 9	0.00	0.00	0 00	0.00	0.00	0 00	0.00	0.00	0.00
Run 10	0.00	0.00	0 00	0 00	0.00	0.00	0.00	0.00	0.00

Figure 3 23 Result Printout with Coefficients only

Embry-Riddle Aeronautical University 2/3/03 3 03 PM
Wind Tunnel Data Acquisition Summary
WINDT2002 v2 0

	AOA (deg)	D (lb)	FY (lb)	L (lb)	MX	MY	MZ	CD	CFY	CL	CMX	CMY	CMZ	V (ft/s)	Temp
Run 1	0 00	-0 02	0 02	0 06	-0 41	0 66	-0 95	-0 66	0 57	1 72	-11 20	18 09	-25 97	67 16	69 83
Run 2	0 00	-0 01	0 02	0 02	-0 08	0 51	-0 95	-0 36	0 63	0 68	-2 17	14 18	-26 58	66 40	69 84
Run 3	0 00	-0 01	0 00	0 07	-0 08	0 53	-0 96	-0 40	0 11	1 95	-2 30	14 82	-27 16	66 25	69 91
Run 4	0 00	-0 05	0 02	0 05	-0 16	0 24	-0 96	-1 44	0 58	1 45	-4 46	6 61	-26 75	66 76	69 98
Run 5	0 00	0 00	0 01	0 03	-0 12	0 63	0 94	-0 02	0 33	0 88	-3 30	18 05	-26 85	65 97	70 13
Run 6	0 00	0 00	0 00	0 00	0 00	0 00	0 00	0 00	0 00	0 00	0 00	0 00	0 00	0 00	0 00
Run 7	0 00	0 00	0 00	0 00	0 00	0 00	0 00	0 00	0 00	0 00	0 00	0 00	0 00	0 00	0 00
Run 8	0 00	0 00	0 00	0 00	0 00	0 00	0 00	0 00	0 00	0 00	0 00	0 00	0 00	0 00	0 00
Run 9	0 00	0 00	0 00	0 00	0 00	0 00	0 00	0 00	0 00	0 00	0 00	0 00	0 00	0 00	0 00
Run 10	0 00	0 00	0 00	0 00	0 00	0 00	0 00	0 00	0 00	0 00	0 00	0 00	0 00	0 00	0 00

Figure 3 24 Result Printout with Loads and Coefficients

However, only the numerical data from the combined final table is saved into a .dat file.

3.7 Calibration

A calibration process must be done to find out the numerical values of the calibration factors for each channel. When the voltage output measured by each channel difference is divided by the respective calibration force or moment, a calibration factor will be obtained. The detailed process by which this is done involves applying different loads while recording the output voltages on all channels. The slope of the straight line plot of loads vs. output voltages is the calibration factor.

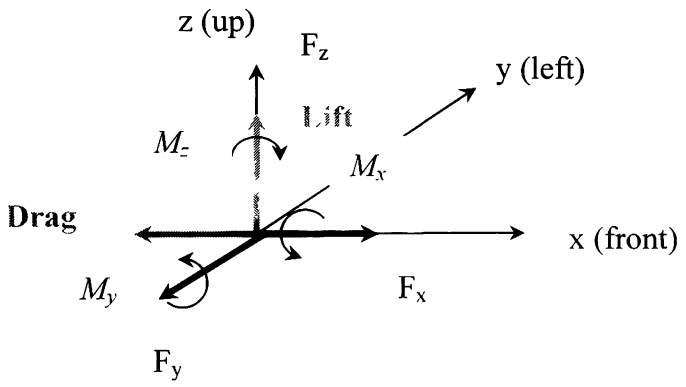

Figure 3.25 Sign Conventions Used in the Program

Table 3.2 Calibration Factor of Force Balance Currently Used

Channel name	Positive sign convention	Calibration factor
Drag	Thrust (F_x or T)	137.7 mv/lb
Side Force	Side Force (F_y)	-110.2 mv/lb
Lift	Lift (F_z or L)	95.9 mv/lb
Rolling Moment	Rolling Moment (M_x)	48.13 mV/in.lb
Pitching Moment	Pitching Moment (M_y)	-36.6 mV/in.lb
Yawing Moment	Yawing Moment (M_z)	-71.3 mV/in.lb

A similar table is located near the top left corner of the main program flow chart.

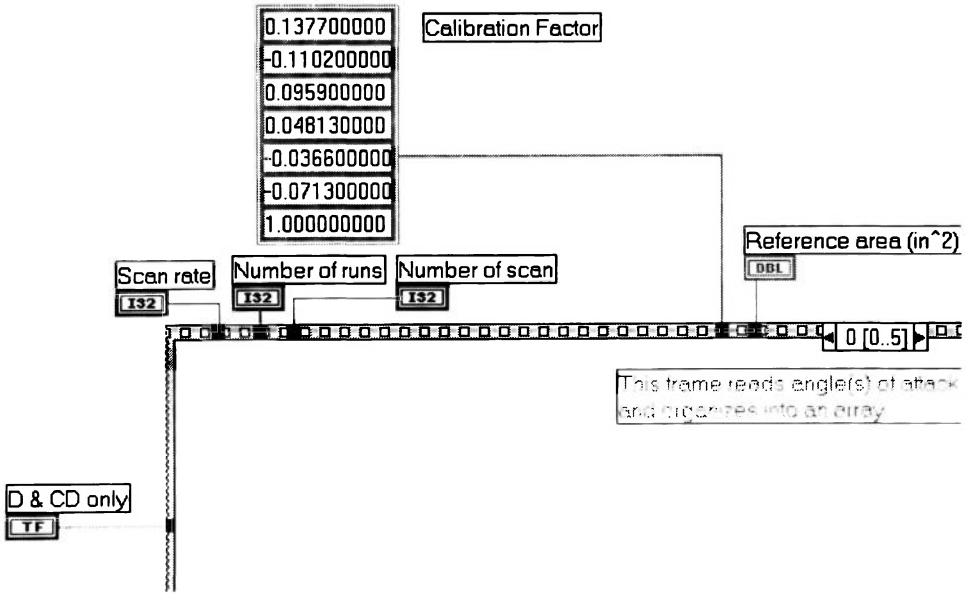

Figure 3.26 Force Balance Calibration Factor Table

Also note that despite being called the Drag channel, a positive drag applied to the balance actually produces a negative voltage output. Therefore, the positive force that this particular channel is measuring is not drag, but the opposite of drag, or thrust. Voltage from the Pitch channel increases as pitching moment (M_y) decreases, therefore

the calibration factor is negative. The calibration factor for the Side Force and Yawing Moment channels are negative is due to the very same reason as well.

Each pressure transducer has a calibration factor. A table containing calibrations for transducer is located at the lower left corner of the flow chart.

Table 3.3 Pressure Transducer Calibration Factors

Pressure transducer number	Calibration factor (in. H_2O/V)
1	442
2	4.30
3	429
4	439
5	439
6	437
7	437
8	426
9	438
10	444

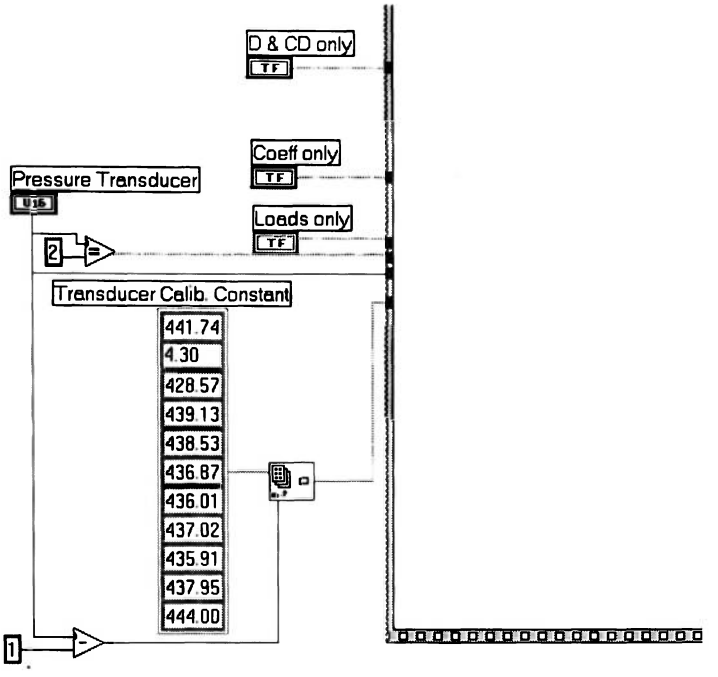

Figure 3.27 Pressure Transducer Calibration Factor Table

The calibration factor of the temperature sensor is simply 10 ^{o}F/V.

CHAPTER 4

Observations Made During Testing

4.1 Signal Amplification

The original balance load cells were not amplified before entering the data acquisition board. For every pound of force exerted, the voltage change is approximately 100 μV.

However, on a 12-bit data acquisition board, the smallest voltage the board can measure is 4.88 mV, if a -10 to +10 V range is used. Measurements that are more precise can be made by the current 12-bit card by using a smaller voltage range or by adding amplifiers to the load cells. If a much smaller range is used, the magnitude of the signal will be very small (in microvolts) so that, external noises picked up along the cables carrying the signal from load cells to the data acquisition board may be large enough to cause inaccurate reading. If the signal is greatly amplified, external noises picked up along the cables will appear insignificant with respect to the signal. Another concern with the such method is that without amplification, the signal may sometimes exceed the voltage limit which the card can read if the voltages are not properly zeroed before the experiment. The zeroing is done manually with dials. If the zero readings were

addicentally allowed to remian very close to or more than the voltage limit which the board is set to read, the active reading would exceed the limit for the channel and system would return a signal that is the maximum reading (which is the limit set on the board) This would effectively lose all data corresponding to the loads are applied to the force balance.

An amplifier with a gain of 1000 was added to each load cell. As a result, the new calibration factors are about 1000 times of the original ones were used before the modifications. The detailed diagram of the amplifier circuit can be found in Appendix D. Each pair of differential signals is amplified and yields single-ended referenced signals. It is then converted into a differential signal before being output to the data acquisition board. The new calibration factors for forces are about 100 mV/lb. With a resolution of 4.88 mV, this means that the new system is accurate enough to tell forces as small as $1/20^{th}$ of a pound (4.88 mV divided by 100 mV/lb). It is not as accurate as the old HP system that was 16-bit. Nevertheless, $1/20^{th}$ of a pound is sufficient for the experiments performed in the lab.

An amplifier with a gain of 100 was added later to one of the pressure transducers to improve the low speed accuracy of the Pitot-static system. The amplifier circuit is similar to those for force balance load cells except it has a built-in hardware filter. The common mode rejection ratio of the amplifier used under ideal condition is 90 dB.

4.2 Different Voltage Range for Pressure Transducer

A vital input for the function AI MULT PT  is the output range. By default, it is set to ±10 Volts. Initially, both output voltages from load cells and pressure transducers were set to this default range. This caused unacceptable resolution in the pressure transducer reading. The smallest difference the system can tell in pressure was about 2 inches of water (from multiplying the calibration factor to 4.88 mV, which is the resolution of ±10 V range). It was later found out that the maximum allowable pressure difference written on the transducer is only equivalent to 0.05 V. The pressure transducer has maximum output range of ±0.8 pounds per square inch.

average calibration factor = 430 in. H_2O/Volt

5.204 in. H_2O = 1 psf

1 psi = 144 psf

max output = 0.8 psi

$$\text{max output voltage} = \frac{0.8 \times 144}{5.204 \times 430}$$
$$= 0.05148 \text{ Volt}$$
$$\approx 0.05 \text{ Volt}$$

That means that the output voltage from transducer will never reach the magnitude of 10V. Unlike the balance which can be subjected (mechanically, according to manufacturer) to loads great enough to generate voltage that reaches 10V, the

transducer is not. Also, the top speed of the wind tunnel is only capable of producing an equivalent of 0.018 V.

$$\text{max recorded dynamic pressure} = 8 \text{ in. } H_2O$$

$$\text{equivalent output voltage} = \frac{8}{430}$$

$$= 0.0186 \text{ Volt}$$

As described before, larger voltage range decreases the accuracy. It was then determined that in the experiments that are conducted, no dynamic pressure more than equivalent to 0.02V is expected. So, the voltage range for pressure transducer was changed to ± 0.02 V. That solved the problem.

As described before, the default transducer currently has an amplifier with a gain of 100. This changes the input range from ±0.02 V to ±2V as shown in Figure 2.3.

4.3 Noise and Interference

A laboratory environment can never be perfectly free of noise and interference to data acquisition. Signals that are not part of the experiment can be picked by the data acquisition system. In most situation, it would be preferable to have filter to take out most of the signals that are not relevant to the experiments. The sources of this "junk" can be external or internal. Currently, the noise and interference in the lab do not pose enough threat to seriously affect the experiments. Therefore there is no comprehensive filtering system (hardware or software) other than the averaging process installed. With

the averaging process alone, the data appears to be very consistent. However, it is important to discuss the effects of and solutions to noise and interference for future reference, if it is decided to have such filter.

The noise and interference covers a huge bandwidth. The most significant noise is from the amplifiers (for load cells and pressure transducers) themselves. The noise is the inherent characteristic of the amplifiers. Other sources of noise can be magnetic. The lab is full of conductors carrying electric currents, thus producing magnetic fields. The electric discharge in fluorescent lighting can interfere as well. The 60 Hz frequency of the alternating current can contribute to interference also, especially when most of the experiments are run at 60 Hz sampling rate. However, there is no sign of improving data consistency with higher sampling rate, which may mean that such interference is insignificant. Since the force balance structure is slightly flexible, sounds can cause it to vibrate, which adds to the signals.

There is another source of interference that is special only to propeller experiments. A ½ horsepower electric motor with a 3-blade propeller is mounted on the force balance to measure the thrust or drag produced. A rather large (about ±0.1 V) sinusoidal waveform is seen on the force balance output. The frequency of that waveform is linearly proportional to the propeller RPM. Each time a propeller blade passes in front of the mounting support, it exerts a notable force on the support. This is believed to be the source of that interference. The following graphs show the waveforms on Drag channel when the propeller was turning, sampling at 1 kHz.

voltage (V)

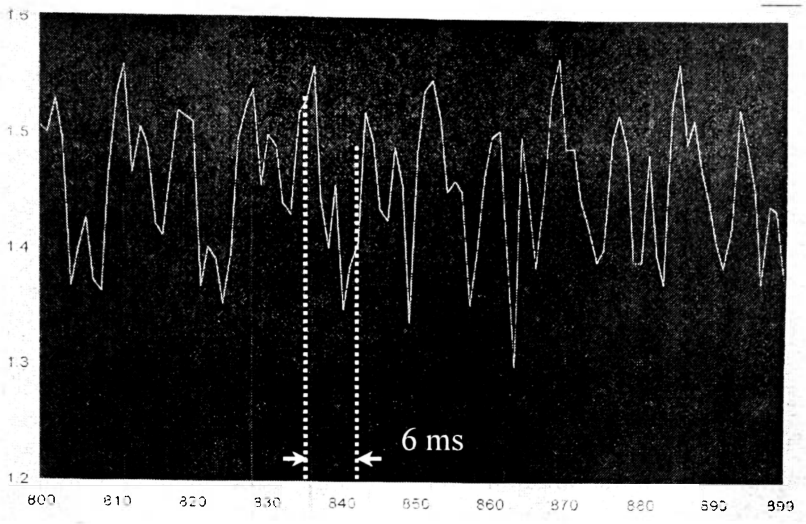

time (ms)

Figure 4.1 Voltage Output from Drag Channel at 3400 RPM

$$\text{blade passage frequency} = \frac{3 \times 3400}{60}$$
$$= 170 \text{ Hz}$$
$$\text{blade passage period} = {}^{1}\!/_{170}$$
$$= 5.9 \text{ ms}$$

Voltage (V)

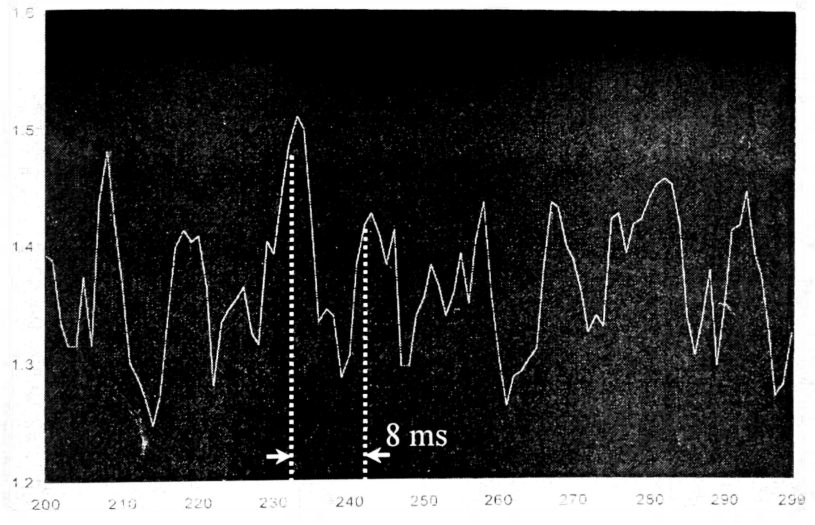

time (ms)

Figure 4.2 Voltage Output from Drag Channel at 2500 RPM

$$\text{blade passage frequency} = \frac{3 \times 2500}{60}$$
$$= 125 \text{ Hz}$$
$$\text{blade passage period} = {}^{1}\!/_{125}$$
$$= 8 \text{ ms}$$

However, since the interference is sinusoidal, the averaging can still make the final result appeared to be very consistent.

CHAPTER 5

Recommendations for the Future

Despite the fact that this data acquisition system has met its requirement to perform the regular experiments well, there are still several minor modifications worth considering for the future to further improve the system's efficiency. More options can be made available to the user in order to expand the capability of the system to accommodate new types of experiments as well.

5.1 Filter Solution

The idea of having a software-based filter in addition to averaging was investigated to assess its feasibility. A special VI called efilt.vi was created to compare unfiltered signal to filtered signal. A low pass elliptical filter was chosen for this job. Since the data taken in all of the wind tunnel experiments are static (near zero frequency), a low cut off frequency of 3 Hz is used. Everything that is over 3 Hz will be excluded. The following graph shows the signals comparison for Drag channel at a sampling rate of 60 Hz.

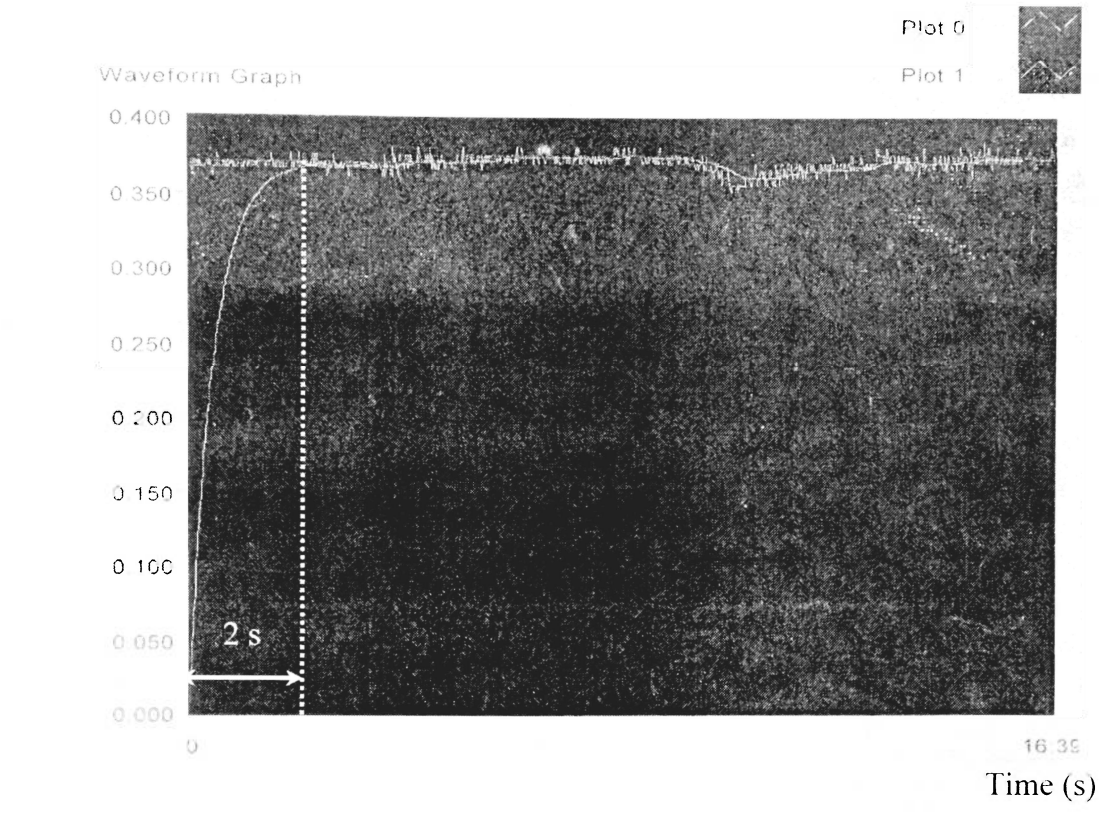

Note: the y-axis is in volt, while the x-axis is time elapsed in second

Figure 5.1 Filter Test

It is found out that with order of one, the elliptical filter can eliminate almost all noise and interference. However, it takes almost 2 seconds to flatten out at a sampling rate of 60 Hz. In a typical 10-run experiment, the 8 channels would be scanned 22 times. The total delay would be (22 times 8 times 2 seconds) 352 seconds, which would make it difficult for the complete experiment to be completed within the time allotted. That time

is dependent of the sampling frequency. At higher sampling frequency, the time it takes to flatten out is less with the same amount of samples.

One way of incorporating the elliptical filter without significant delay is by increasing the sampling rate from 60 Hz to possibly 1000 Hz. 60 Hz itself is not the best sampling frequency due to possible power line interference. Another way is by reducing the number of samples. If the elliptical filter works out fine, there may not be any need for a large number of samples for averaging to provide consistent data.

5.2 Order of Running the Experiment

Almost all of the experiments done with the system regularly involve multiple runs. Currently with WINDT2002, the user has to perform the active data taking in the same order in which the weight tares are taken. For example, if there are 8 runs in the experiment, the weight tares have to be taken 8 times. Then the user has to finish taking all 8 active runs in the same order before outputting the result.

However, the old system (written in BASIC) actually allowed the user to perform the active data taking in a different order than the order in which the weight tares were taken. The order could be reversed or arbitrary. The user could also choose to end the program without finishing all of the 8 active runs. This is because the structures of the old and new system are significantly different.

The old system basically tied each of the weight tare with an angle of attack. During the actual data process, the user specified an angle of attack value and the corresponding weight tare was retrieved and then used. The new system stores everything in arrays and always starts from the first row to the last. The weight tare taken first would be put into the first row of weight tare array and so on. The first active data taken will only use the first weight tare taken and so forth. The angle of attack values only serve to remind the user what run is currently being executed. In addition, the old system allowed the user to use a single weight tare for different active runs taken at same angle of attack. However, in the new system, the user has to do 8 weight tares for 8 runs taken at the same angle of attack. This slows down the whole process.

The reason for choosing this structure over the old one is software efficiency. The old system had to go through at table look-up process in order to find out the corresponding weight tare. If that corresponding weight tare was taken last, the system would have to go through every single entry in the whole weight tare file. The new system will always go straight for the n^{th} row of weight tare file when the n^{th} actual data being taken, without going through all the rows.

However, minor changes can be made to the program to allow the user to choose to have reverse order or having a single weight tare for different runs.

5.3 Print Out Format

Currently, as soon as each experiment is completed by the system, the result will be printed on a single piece of paper. However, since most of the experiments performed regularly have less than 10 runs, only a small portion (less than 1/3) of the paper is actually printed. Some lab sessions have at least 5 experiments, which translates into 5 print outs, on 5 pieces of paper. It seems to be a waste for every student to be given 5 sheets of print out , if there is a way to print the results of all 5 experiments on one single piece of paper.

A simple change in the program can allow the user to choose which part of the paper in which the result will be printed on. For a 5 experiments session, the user will perform the first experiment and print the result on the top 1/3 of the paper. Then the user will reload the printed paper, and proceed with the second experiment. After it is completed, the result will be printed on the middle 1/3 of the paper. The paper is then reloaded and the third experiment is performed. After that, the result is printed on the bottom 1/3 of the paper. The user can then repeat with the reverse side. This implementation can significantly reduce the amount of paper being used by the system.

5.4 Variable Force Balance Voltage Range

The maximum force the system can measure is about 100 pounds, which is equivalent to 10 volts of output. This is why ±10 volts was chosen for the output range

for the force balance channels. But what if there is an experiment in which the maximum load applied never exceeds 10 pounds? In that case, it would be favorable to use a small range such as ±1 volt to give a better resolution. With that new range, the new resolution is now 488 microvolts instead of 4.88 millivolts. That means the system can now detect force as small as 1/200 of a pound instead of 1/20 of a pound.

A knob or dial could be placed on the front panel for the user to input the maximum expected load of the experiment. The system will then calculate the best range based on the maximum expected load to yield the optimum resolution. This would give the system the ability to perform very precise measure for experiments with small loads.

CHAPTER 6

Sample Experiments

In order to demonstrate that the data acquisition system functions properly, sample data from 3 experiments regularly performed in AE309 with the Data Acquisition System is shown below.

6.1 Experiment 8 Drag of Streamlined Bodies of Revolution

6.11 Introduction

The purpose of this experiment is to find out the relationship between the length of a family of streamlined bodies of the same diameter and zero-lift drag. There are 7 of the bodies, fineness ratio (l/d) ranging from 0.083 to 8. The first one is a flat plate, while the rest are teardrop like. They all have six inches diameter.

The zero-lift drag of a body is affected by 2 factors. It increases with the wetted surface area as bigger area produces more skin friction. This is evident on bodies of larger fineness ratio. Drag is also heavily affected by separated flow. A

separated wake can create an pressure difference between front and back of the body, resulting in drag. This is evident in the flat plate body. By summing skin friction drag and pressure drag, we will have a drag function with a minimum value.

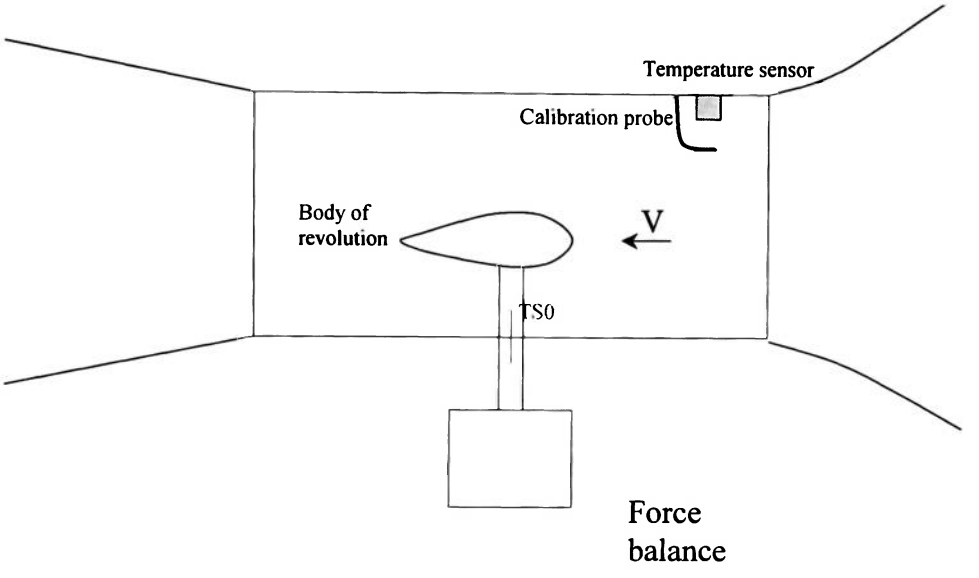

Figure 6.1 Experiment 8 Set Up

6.12 Measured Data

Table 6.1 Measured Drag Data

l/d	C_D
0.083	1.24
1	0.27
2	0.14
3	0.08
4	0.09
5	0.11
8	0.15

6.13 Final Data

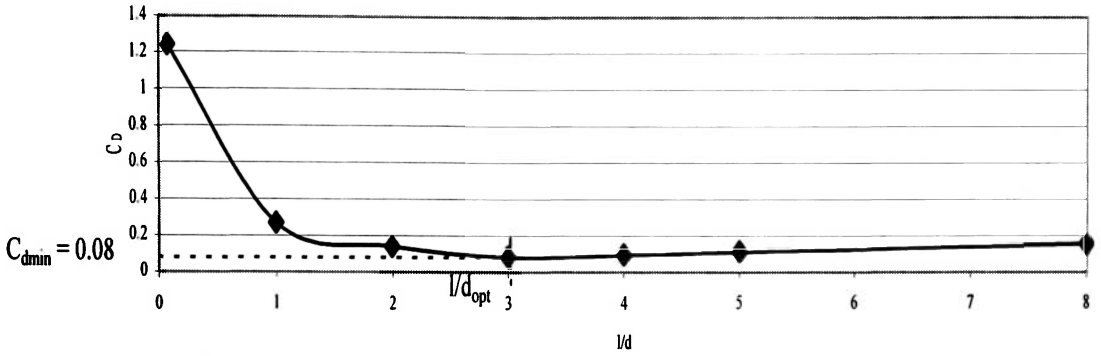

Figure 6.2 Zero-lift Drag vs. Fineness Ratio

6.14 Conclusion

It was found out that the 2 lowest fineness ratio models did have the greatest drag. However, the rest of the models have very close values to each other. Fineness ratio of 3 recorded the lowest coefficient of drag at 0.08, followed by fineness ratio of 4 at 0.09. The precision of the balance is only marginally acceptable for measure the small forces experienced in the higher fineness ration bodies (approximately 0.3 pounds) and a more precise measure device is being developed for future use.

6.2 Experiment 9A Wing/fuselage/tail Model Buildup

6.2.1 Introduction

This experiment evaluates the aerodynamic characteristic of a 3-dimensional wing and a complete aircraft model of "Viper"(a general aviation aircraft designed in AE420 class). The coefficients measured are coefficient of lift, drag and pitching moment. The 5 different runs of this experiment will be conducted with wing alone, fuselage added, tail added, tail incidence angle changed and finally landing gear added.

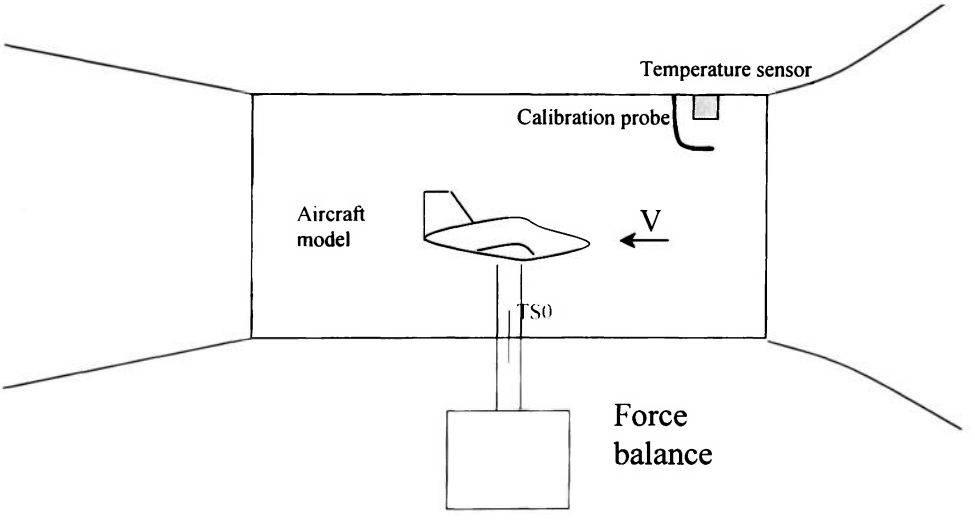

Figure 6.3 Experiment 9A Set Up

The lift curve should exhibit a hook shaped profile, with a significant linear section before reaching stall.

The wing alone should be marginally stable, as shown as in the coefficient of moment plot. With the fuselage, it becomes unstable. However, with the horizontal tail added, it becomes stable, with negative slope on the plot.

6.2.2 Measured Data

Table 6.2 Measured Data, Wing Alone

α (deg)	C_L	C_D	C_M
-5	-0.36	0.04	-0.04
0	-0.03	0.02	-0.06
5	0.32	0.02	-0.05
10	0.67	0.02	-0.08
12	0.83	0.03	-0.08
14	0.95	0.04	-0.08
16	0.91	0.06	-0.09
18	0.95	0.14	-0.06

Table 6.3 Measured Data, Wing and Fuselage

α (deg)	C_L	C_D	C_M
-5	-0.42	0.07	-0.12
0	-0.05	0.03	-0.06
5	0.42	0.02	-0.04
10	0.73	0.03	-0.03
12	0.87	0.05	-0.04
14	1.08	0.08	0.00
16	0.86	0.12	0.01
18	1.06	0.14	0.07

Table 6.4 Measured Data, Wing, Fuselage and Tail

α (deg)	C_L	C_D	C_M
-5	-0.39	0.04	0.31
0	0.00	0.03	0.04
5	0.42	0.03	-0.15
10	0.78	0.04	-0.27
12	0.93	0.05	-0.28
14	0.99	0.06	-0.36
16	0.99	0.08	-0.40
18	1.07	0.14	-0.49

Table 6.5 Measured Data, Wing, Fuselage and Tail Incidence = -5^{o}

α (deg)	C_L	C_D	C_M
-5	-0.42	0.04	0.40
0	0.03	0.03	0.23
5	0.51	0.03	0.09
10	0.74	0.04	-0.07
12	0.90	0.06	-0.17
14	1.02	0.06	-0.24
16	1.02	0.09	-0.23
18	1.04	0.14	-0.39

Table 6.6 Measured Data, Wing, Fuselage and Tail Incidence = -5° and Landing Gear

α (deg)	C_L	C_D	C_M
-5	-0.36	0.09	0.44
0	0.03	0.04	0.27
5	0.52	0.04	0.10
10	0.84	0.06	-0.08
12	0.88	0.08	-0.16
14	0.95	0.08	-0.21
16	0.89	0.13	-0.20
18	1.01	0.18	-0.27

5.2.3 Final Data

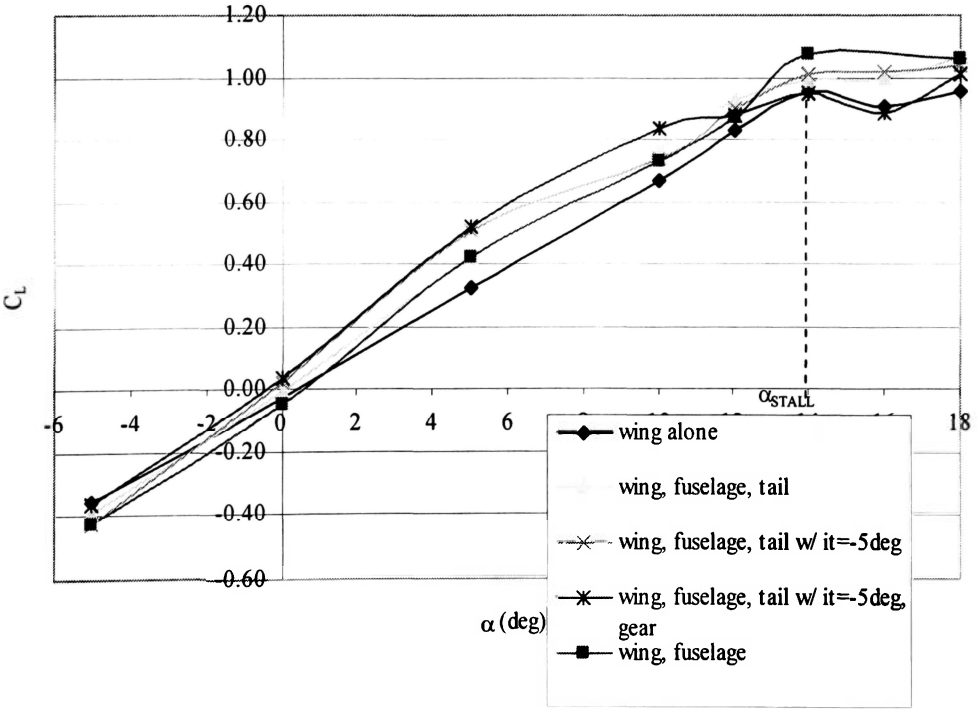

Figure 6.4 Coefficient of Lift vs. Angle of Attack

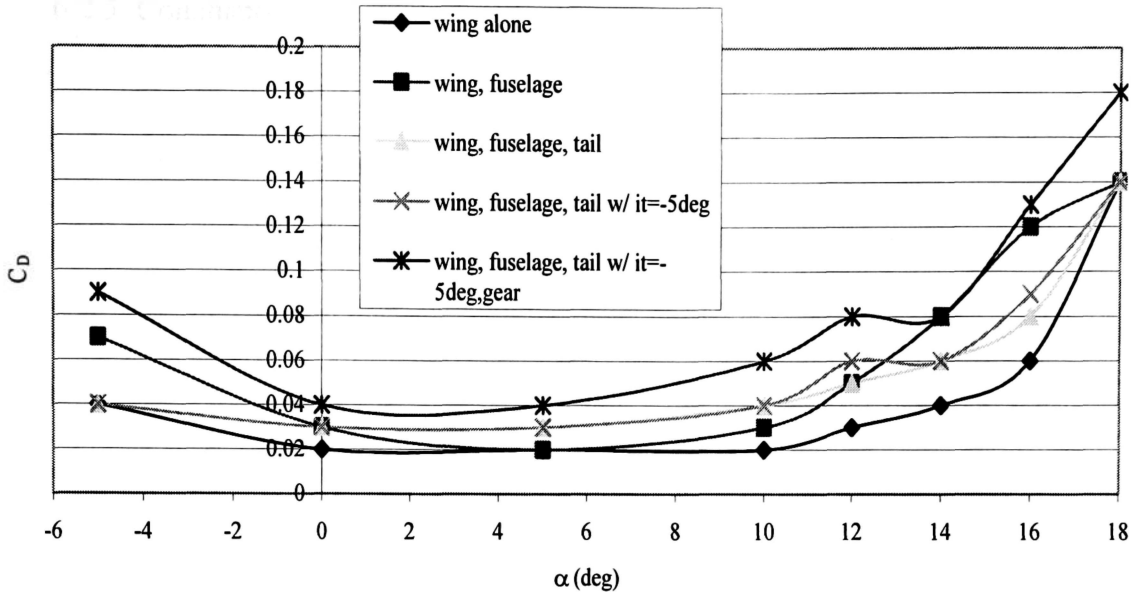

Figure 6.5 Coefficient of Drag vs. Angle of Attack

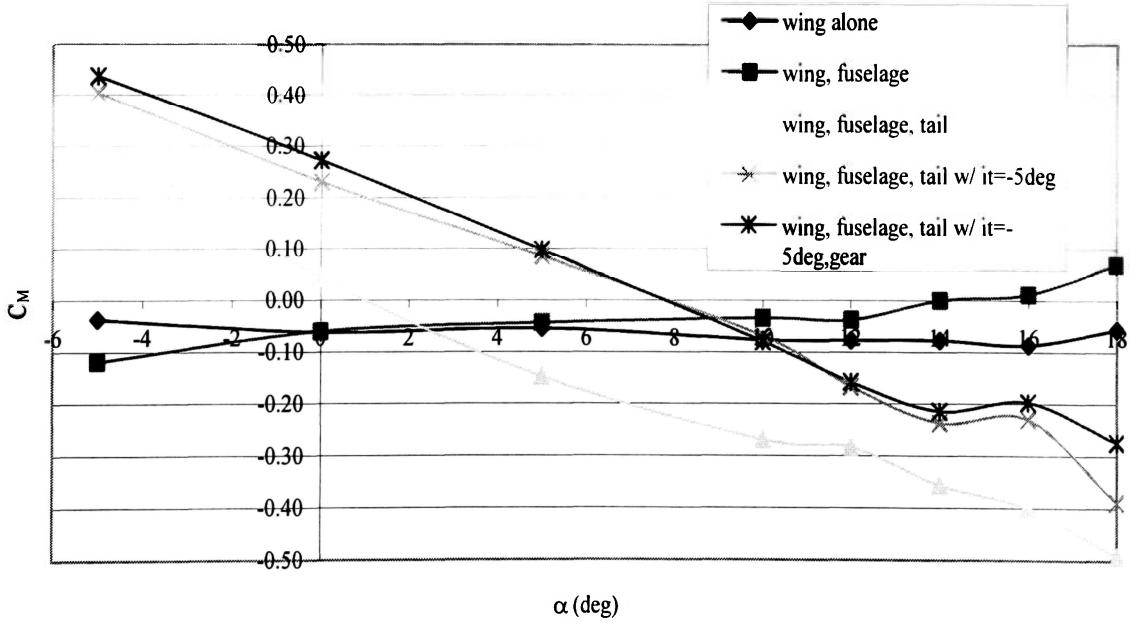

Figure 6.6 Coefficient of Pitching Moment vs. Angle of Attack

6.2.3 Conclusion

As seen from Figure 6.2, all 5 lift curves have the hook shaped profile, and significant linear section before stall. Also notable is the wing alone generates less lift than the combinations with fuselage added.

As seen from Figure 6.3, all drag curves have the U-shaped profile. Large amount of drag is seen after the stall due to separation. Also notable is the landing gear does produce a significant amount of drag as compared to without landing gear.

As seen from Figure 6.4, several observations are made. As predicted, the wing alone is marginally stable, with almost zero slope. However, the wing and fuselage combination is slightly unstable, as shown by the positive slope. The addition of horizontal tail makes it stable, as shown by the negative slopes of the last 3 configurations. Also notable is the change of incidence angle of tail nose down produces a nose up moment, which shifts the curve up by an amount.

6.3 Experiment 11 Propeller Performance

6.3.1 Introduction

A propeller blade is basically a rotating airfoil. The airfoil section is positioned at a positive angle of attack to produce lift. The lift by each section can be summed up as thrust of the entire propeller blade.

Several factors affect propeller performance, including blade pitch angle (β), RPM and freestream velocity. Pitch angle is the angle between the rotational plane and the chord line of the blade airfoil section. The amount of local resultant velocity (summation from rotational velocity and freestream velocity) also determines the amount of lift generated by that section.

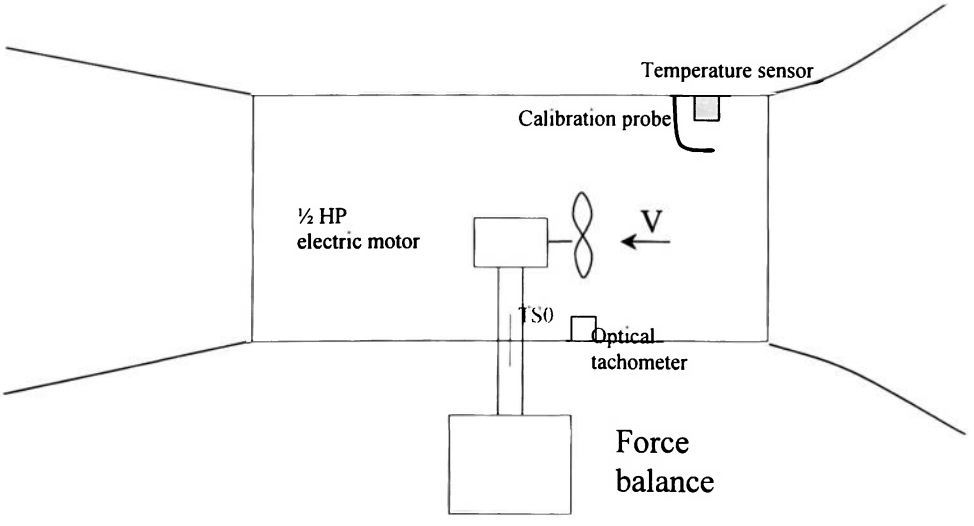

Figure 6.7 Experiment 11 Set Up

6.3.2 Measured Data

Table 6.7 Measured Data, Static, Low β

Power (W)	RPM	Thrust (lbs)
50	3296	0.33
100	4499	0.80
150	5330	1.40
200	5913	1.65
250	6541	2.10
300	6911	2.48

Table 6.8 Measured Data, Static, High β

Power (W)	RPM	Thrust (lbs)
50	2869	0.30
100	4030	0.72
150	4684	1.47
200	5380	1.81
250	5768	1.98
300	6234	2.48

Table 6.9 Measured Data, Variable Velocity, High β

Velocity (ft/s)	RPM	Thrust (lbs)
46.64	6360	1.63
92.9	7713	0.71
122.99	9163	0.20
142.79	9610	-0.48

Table 6.10 Measured Data, Variable Velocity, Power off, High β

Velocity (ft/s)	RPM	Thrust (lbs)
50.9	1634	-0.18
90.61	5583	-0.79
121.01	7311	-1.32
142.41	8595	-1.60

6.3.4 Final Data

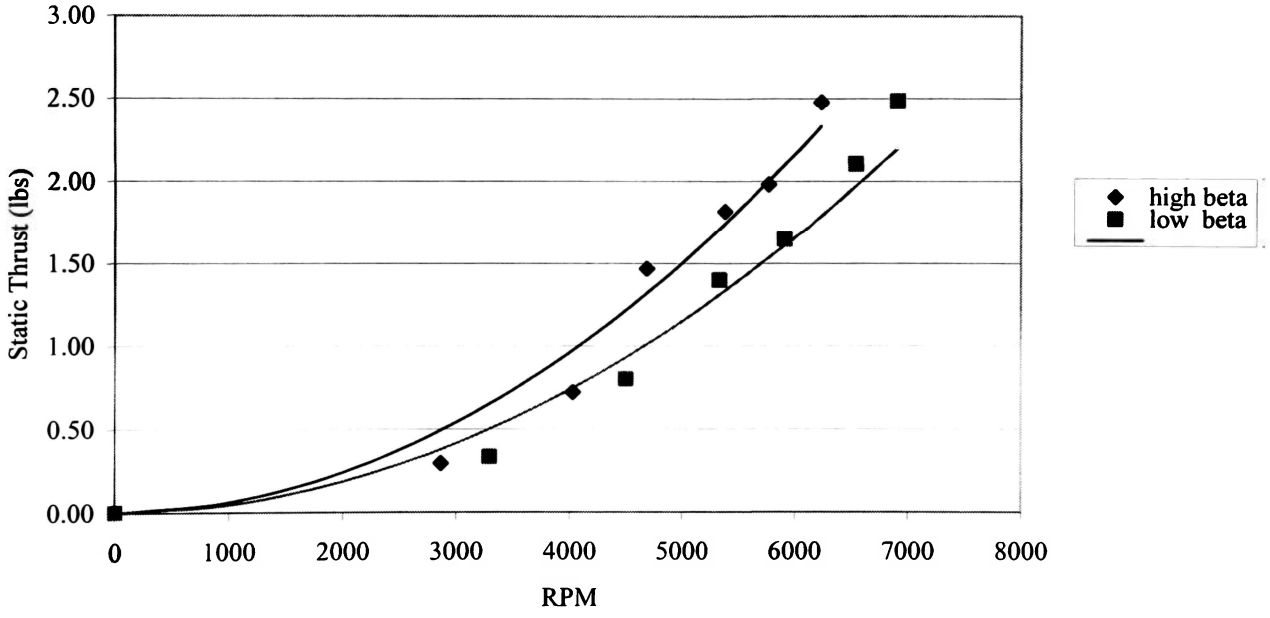

Figure 5.8 Static Thrust vs. RPM

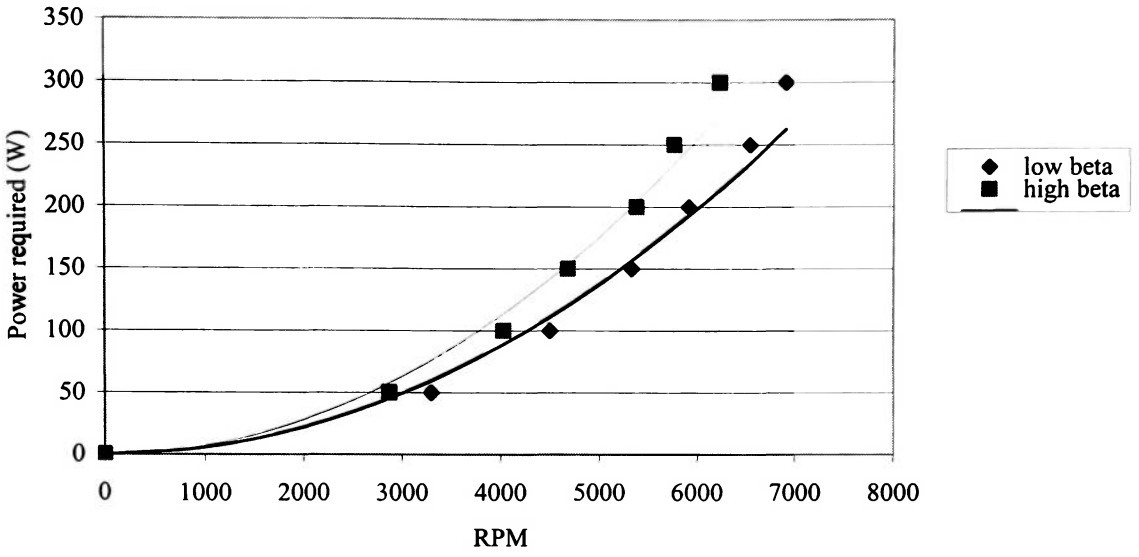

Figure 6.9 Static Power Required vs. RPM

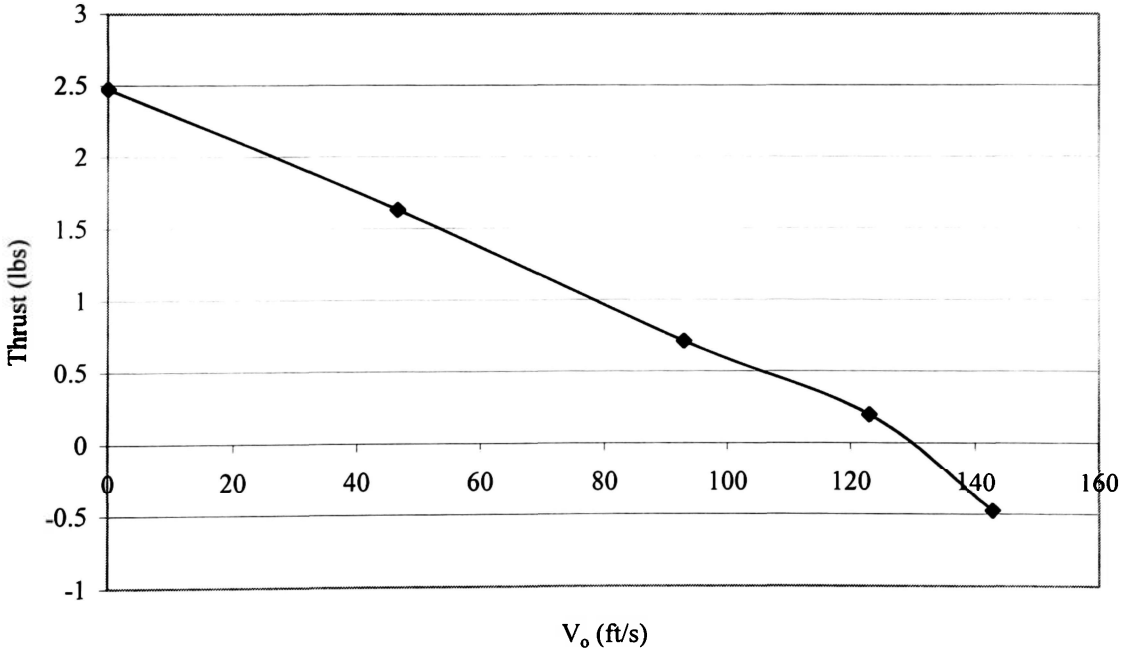

Figure 6.10 Thrust vs. V_o at Constant Power

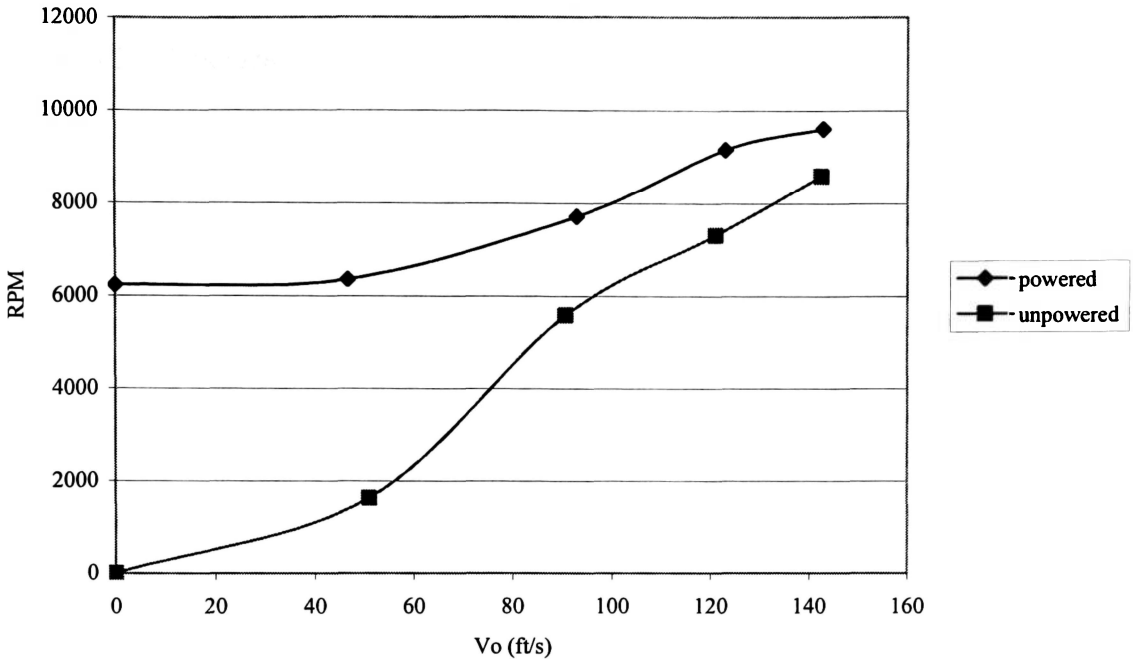

Figure 6.11 RPM vs. V_o at with Power off

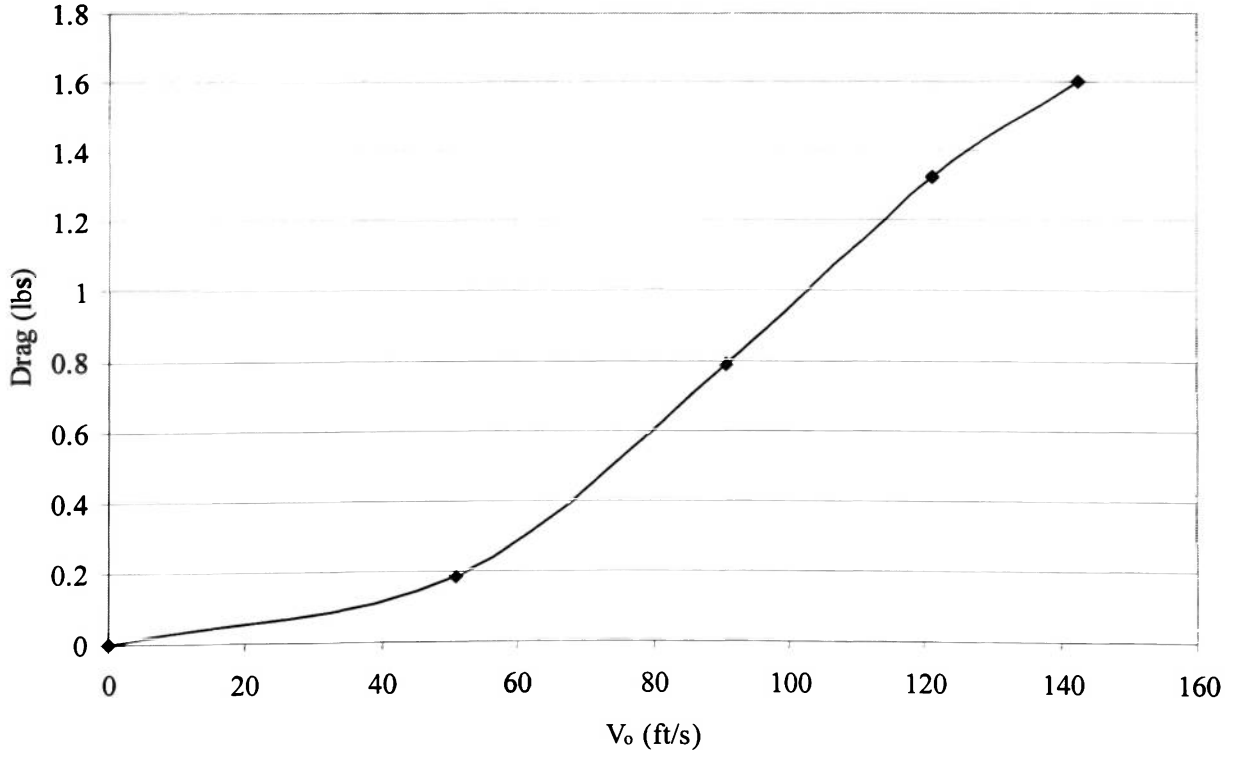

Figure 6.12 Drag vs. V_o at Power off

6.3.5 Conclusion

As shown in Figure 6.5, the static thrust has a parabolic relationship with the RPM. Also, higher pitch produces more thrust at the same RPM than low pitch.

From Figure 6.6, it is shown that higher pitch propeller is harder to turn than lower pitch. That is because the power required to turn the propeller is a function of the drag produced by blade sections. Higher pitch angle makes more lift but at the same time also produces more drag.

Figure 6.7 shows that thrust produced decreases as freestream velocity goes up. At some point, the thrust becomes drag.

From Figure 6.8, it is shown at RPM increases as the freestream velocity increases. Unpowered propeller turns slower than the powered one.

Figure 6.9 shows that wind milling propeller only produces drag, since there is no power input to the propeller.

REFERENCES

1. "Low-speed Wind Tunnel Testing", Jewel B. Barlow, William H. Rae and Alan Pope, Wiley, 1999.
2. "Experimental Aerodynamics and Wind Tunnels", Charles N. Eastlake, Embry-Riddle Aeronautical University, 1998.
3. "Fundamentals of Aerodynamics", John D. Anderson Jr., McGraw-Hill, 1991.
4. "PCI E Series User Manual: Multifunction I/O Devices for PCI Bus Computers", National Instrument, 2002.
5. "DAQ: SCB-68 68-Pin Shielded Connector Block User Manual", National Instrument, 2002.
6. "Validyne Engineering Corporation Products and Capabilities Catalog", Validyne Engineering, 1981.

APPENDIX A

Diagram Legend

Value Input from Front Panel or Passed from Other vi (similar box with values in it is a constant value)


Double Precision Floating Point


Long Integer, 32 bit


Boolean Constant


File Constant


Character Constant

Types of Data

Floating Point

Floating, 1-Dimensional Array

Floating, 2-Dimensional Array

Integer

Boolean

File Path

Character String

Character String, 1-Dimensional Array

Character String, 2-Dimensional Array

Mathematical Functions


Add


Subtract


Multiply


Division


Greater or Equal?


Equal to


Summation


And

Character string manipulations


Format Integer into String


Concatenate Strings


Format Floating into String

Array Functions


Replace Array Element


Index Array


Transpose 2-D Array


Joint arrays


2-D to 1-D Array

Report Functions


New Report


Set Report Font


Append Num Table to Report


Set Report Orientation


Set Report Header Text


Print Report

File Functions


Write Character to File


Write Spreadsheet to File


Read from Spreadsheet File

Miscellaneous Functions


Get Date/Time String


One Button Dialog


Two Button Dialog


AI Acquire Waveforms


Median Filter

Custom made subVIs


acq8chan.vi (acquire voltages from 6 channels from force balance, 1 channel from pressure transducer and 1 channel from temperature sensor)


MT.vi (do moment transfer to 3 moments of different directions)


replacecolumn.vi (replace a column of a 2-D array with another column)


velocity.vi (calculate velocity with voltages from pressure transducer and temperature sensor)

Loop, case & sequence structures

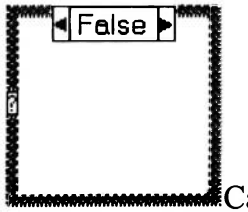

Case

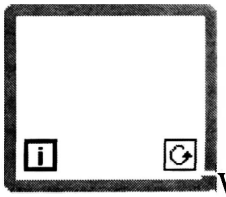
While loop

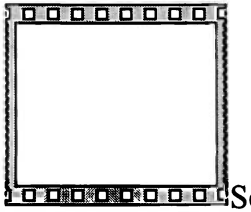
Sequence

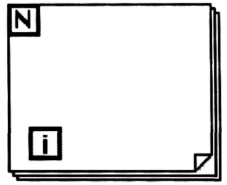

For loop

APPENDIX B
Overall Diagram **with Sequence 0**

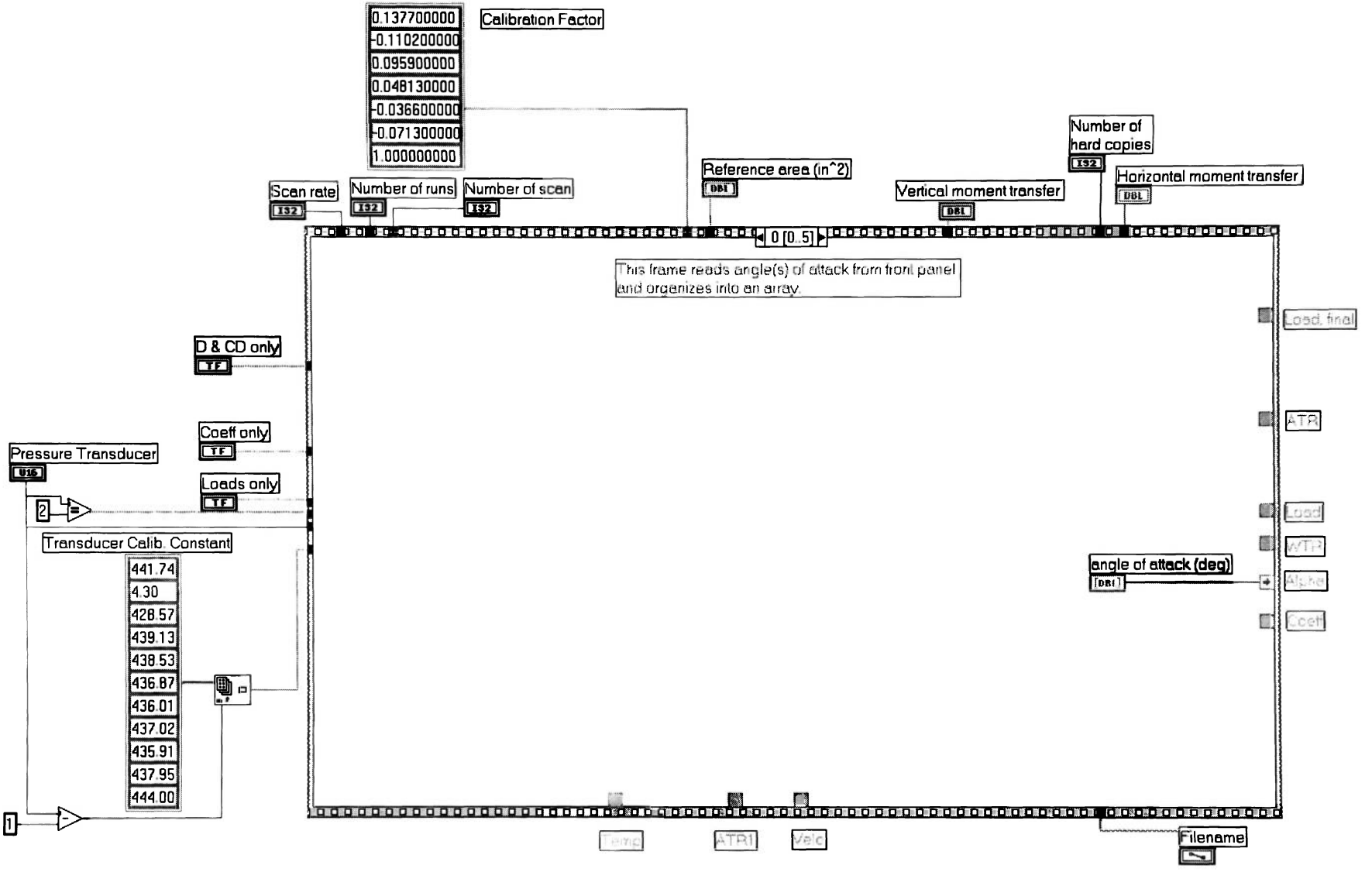

Sequence 1

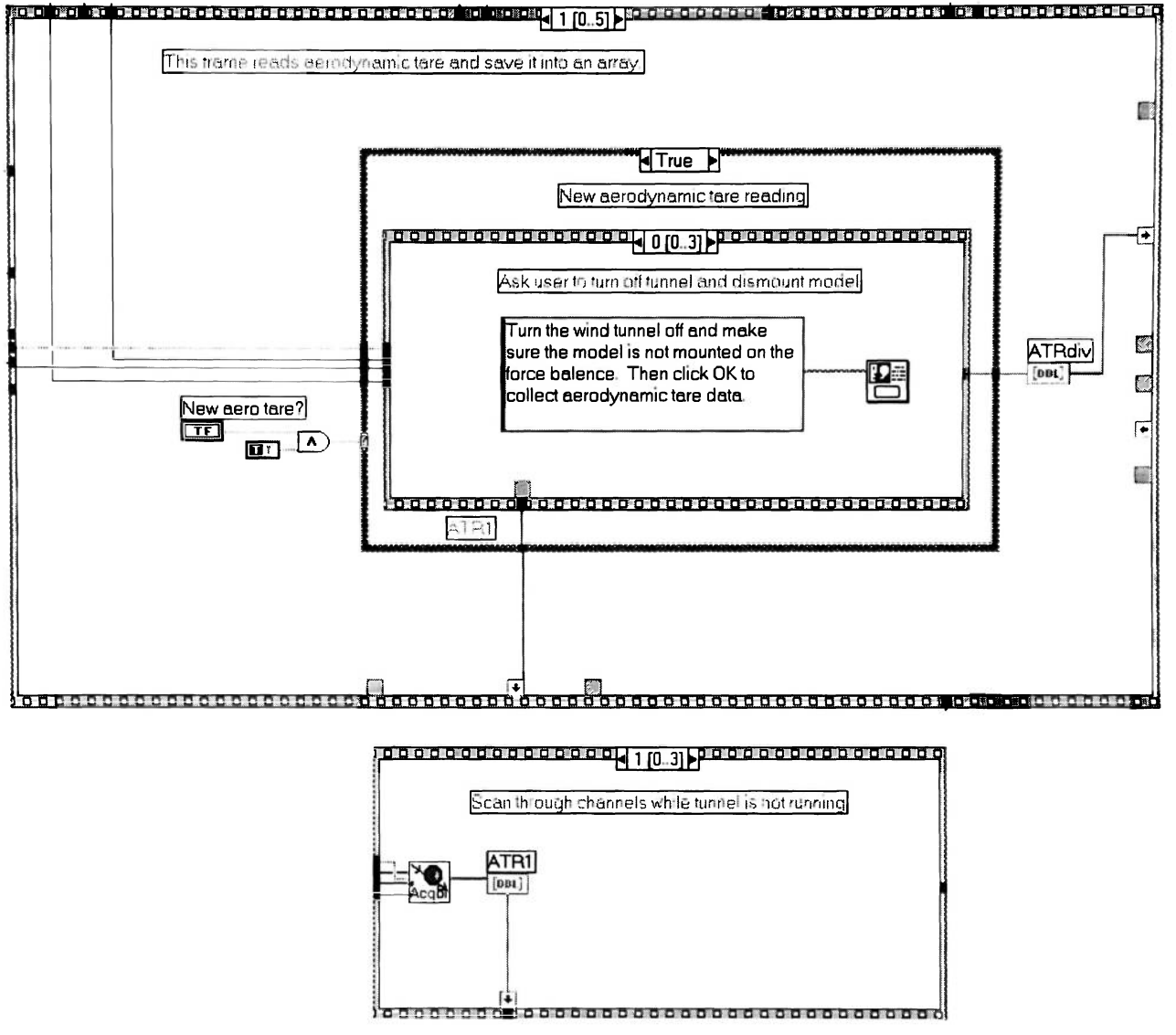
1 [0..5]
This frame reads aerodynamic tare and save it into an array
True
New aerodynamic tare reading
0 [0..3]
Ask user to turn off tunnel and dismount model
Turn the wind tunnel off and make sure the model is not mounted on the force balence. Then click OK to collect aerodynamic tare data.
ATRdiv
DBL
New aero tare?
TF
TT
ATR1
1 [0..3]
Scan through channels while tunnel is not running
ATR1
DBL
Acq

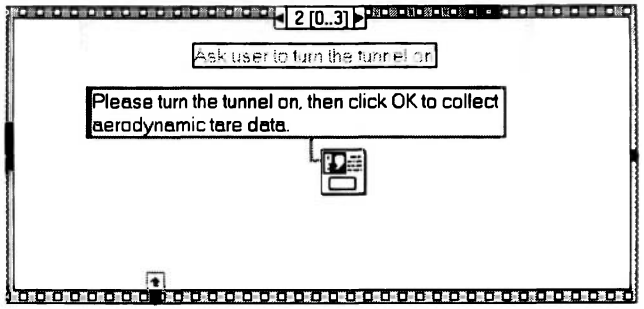
2 [0..3]
Ask user to turn the tunnel on
Please turn the tunnel on, then click OK to collect aerodynamic tare data.

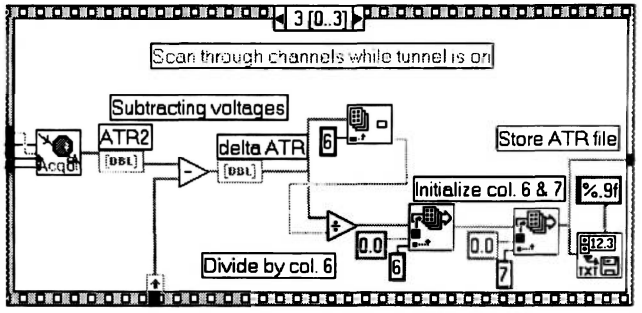
3 [0..3]
Scan through channels while tunnel is on
Subtracting voltages
ATR2
[DBL]
delta ATR
[DBL]
6
Store ATR file
Initialize col. 6 & 7
%.9f
0.0
6
0.0
7
Divide by col. 6

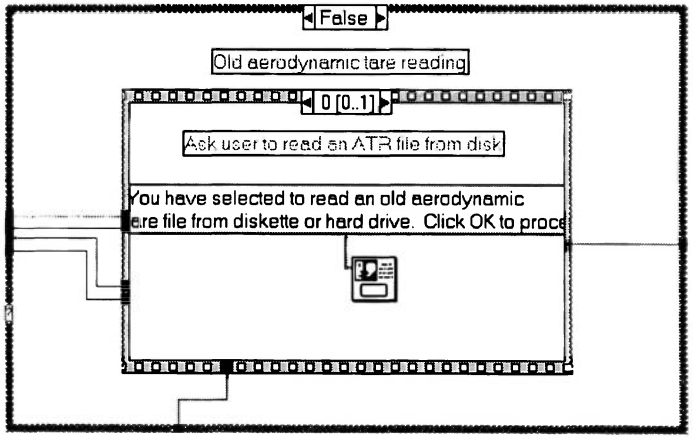
False
Old aerodynamic tare reading
0 [0..1]
Ask user to read an ATR file from disk
You have selected to read an old aerodynamic
are file from diskette or hard drive. Click OK to proce

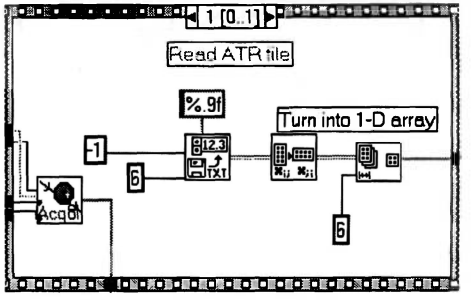
1 [0..1]
Read ATR file
%.9f
Turn into 1-D array
-1
6
Acq0
6

Sequence 2

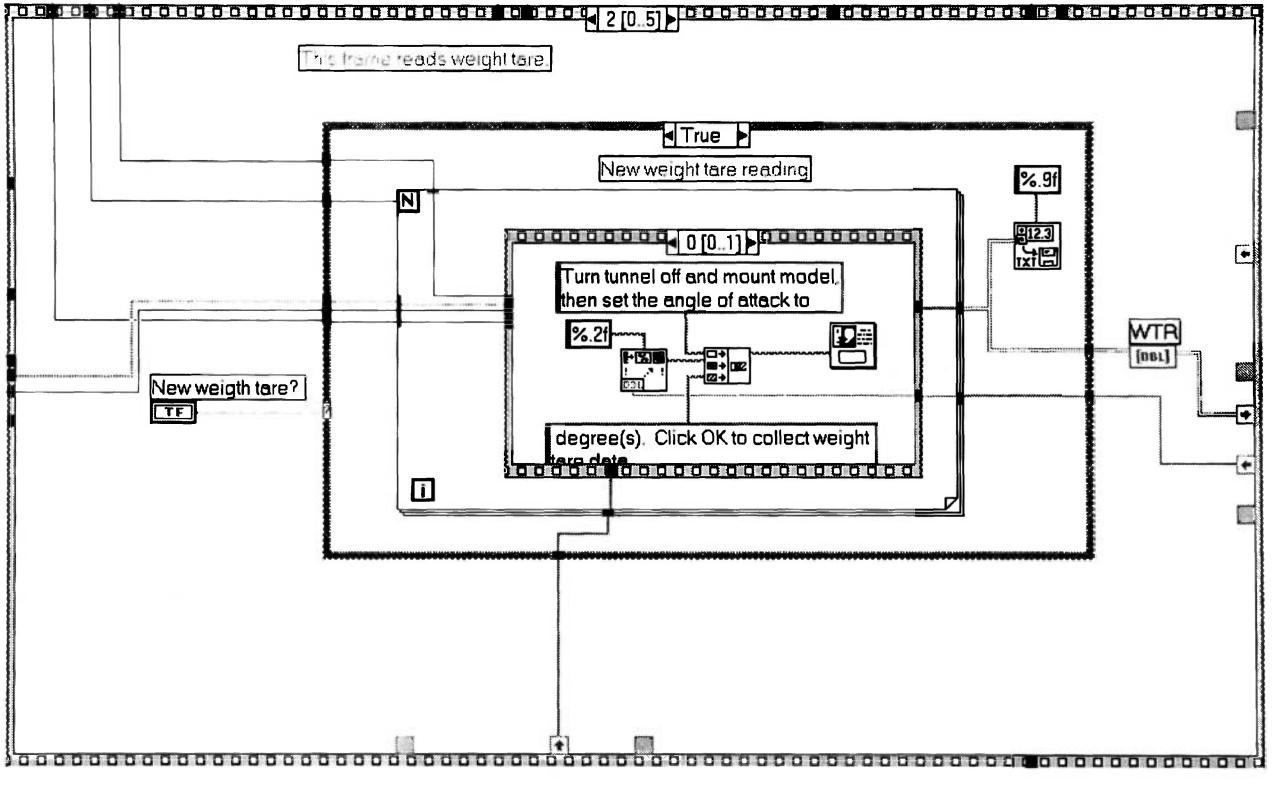
2 [0..5]
This frame reads weight tare
True
New weight tare reading
N
0 [0..1]
Turn tunnel off and mount model, then set the angle of attack to
%.2f
%.9f
WTR
[DBL]
New weigth tare?
TF
degree(s). Click OK to collect weight
i

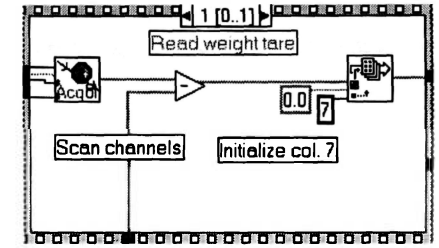
1 [0..1]
Read weight tare
Acq 0
0.0
7
Scan channels
Initialize col. 7

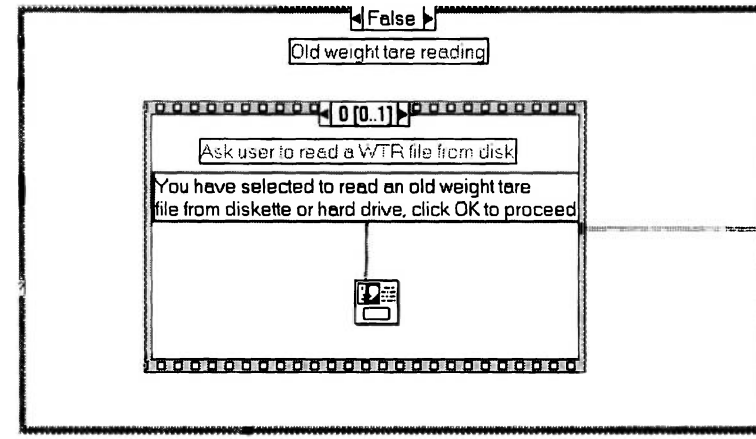
False
Old weight tare reading
0 [0..1]
Ask user to read a WTR file from disk
You have selected to read an old weight tare
file from diskette or hard drive, click OK to proceed

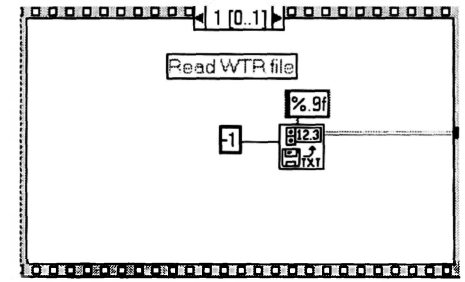
1 [0..1]
Read WTR file
%.9f
-1
123
TXT

Sequence 3

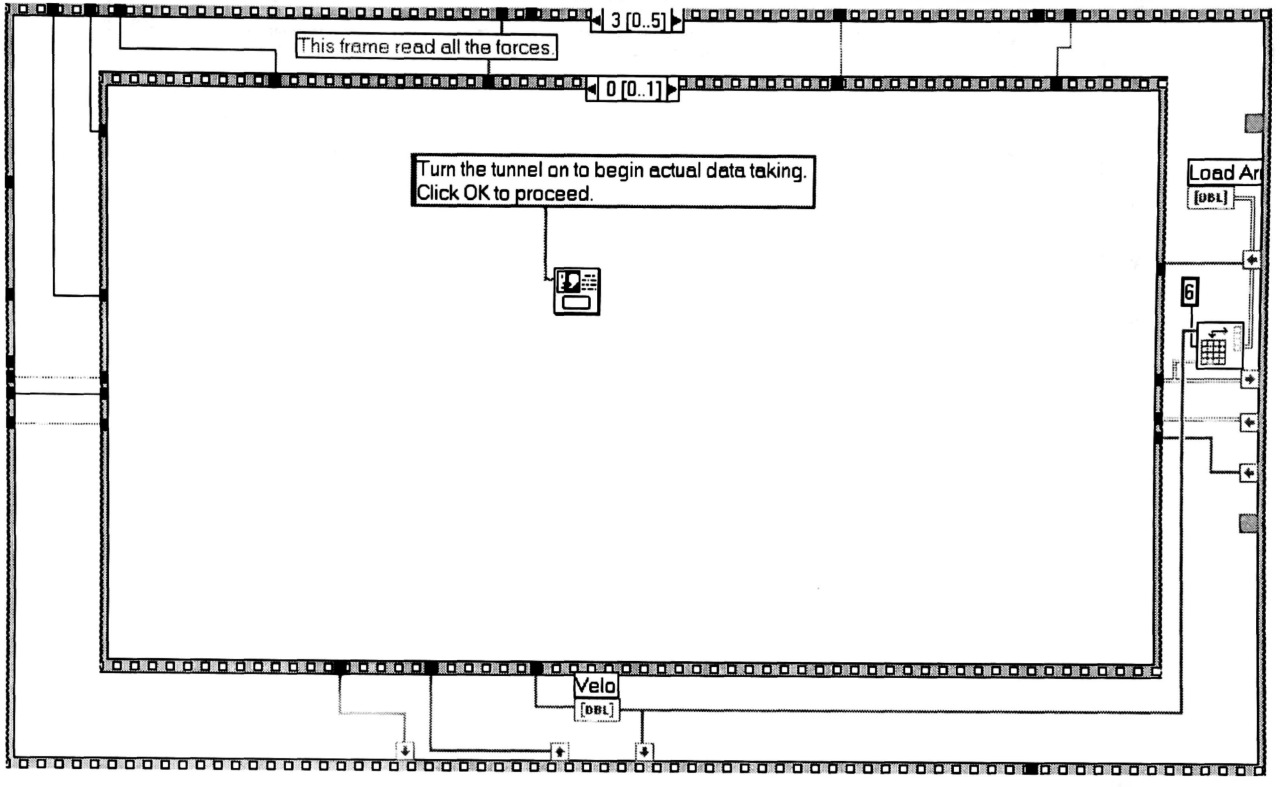
3 [0..5]
This frame read all the forces.
0 [0..1]
Turn the tunnel on to begin actual data taking.
Click OK to proceed.
Load Ar
[DBL]
6
Velo
[DBL]

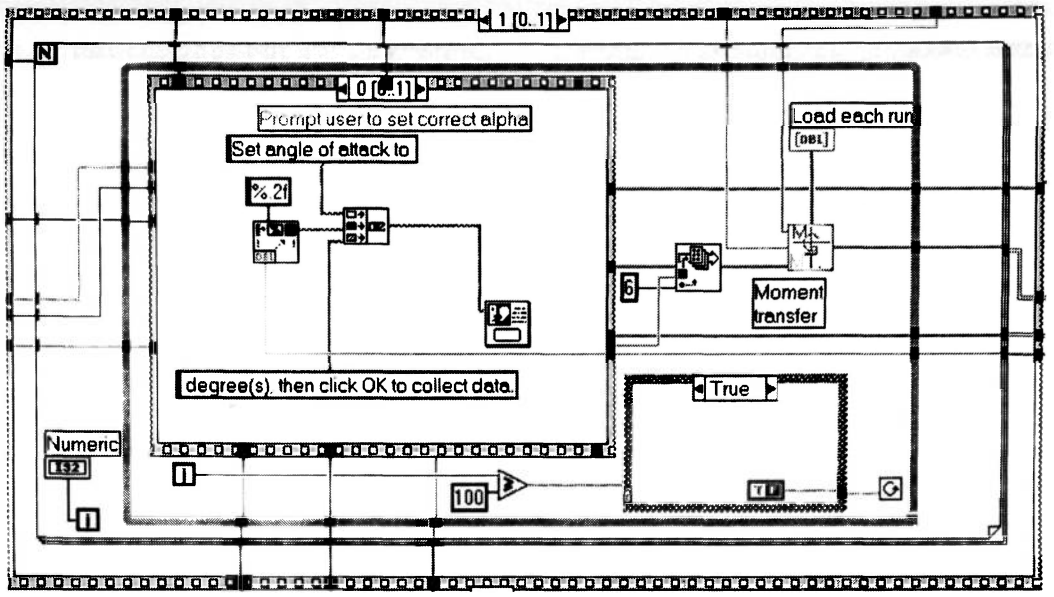
1 [0..1]
N
0 [0..1]
Prompt user to set correct alpha
Set angle of attack to
% 2f
degree(s), then click OK to collect data.
Load each run
[DBL]
Moment
transfer
6
True
Numeric
I32
100

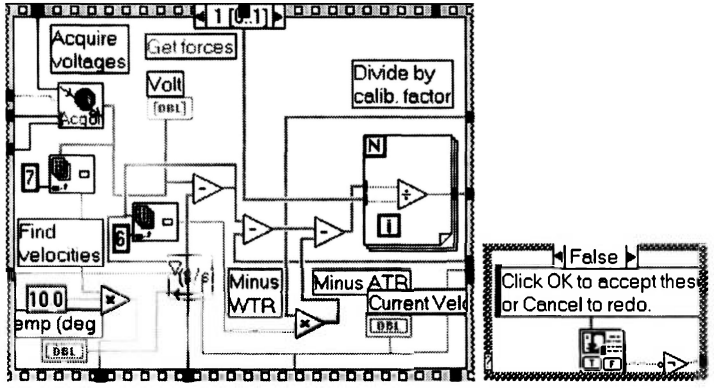
1 [0..1]
Acquire
voltages
Get forces
Volt
[DBL]
Divide by
calib. factor
N
7
6
Find
velocities
Minus
WTR
Minus ATR
Current Vel
[DBL]
100
emp (deg
[DBL]
False
Click OK to accept thes
or Cancel to redo.

Sequence 4

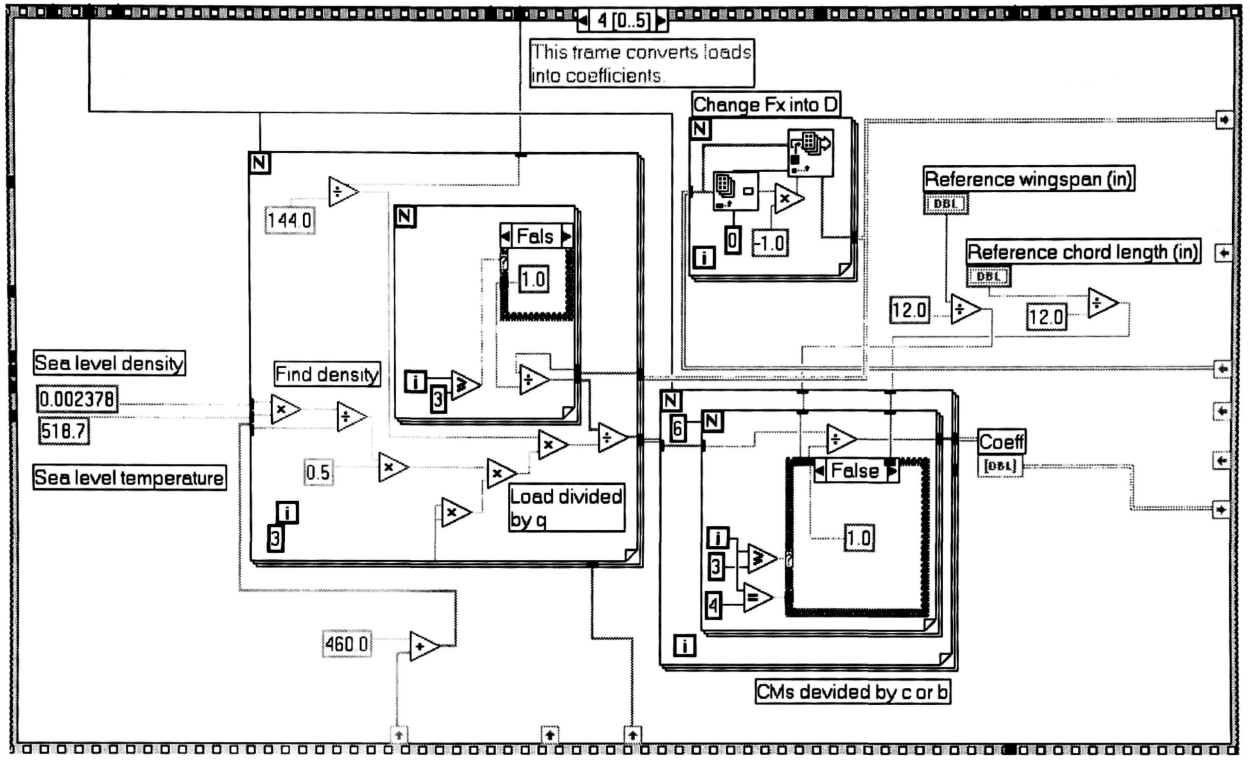
4 [0..5]
This frame converts loads into coefficients
Change Fx into D
Reference wingspan (in)
DBL
Reference chord length (in)
DBL
12.0
12.0
144.0
Fals
1.0
Sea level density
0.002378
518.7
Sea level temperature
Find density
0.5
Load divided by q
460.0
False
1.0
Coeff
DBL
CMs devided by c or b

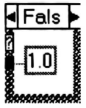
Fals
1.0

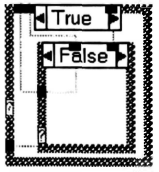
True
False

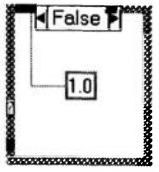
False
1.0

Sequence 5

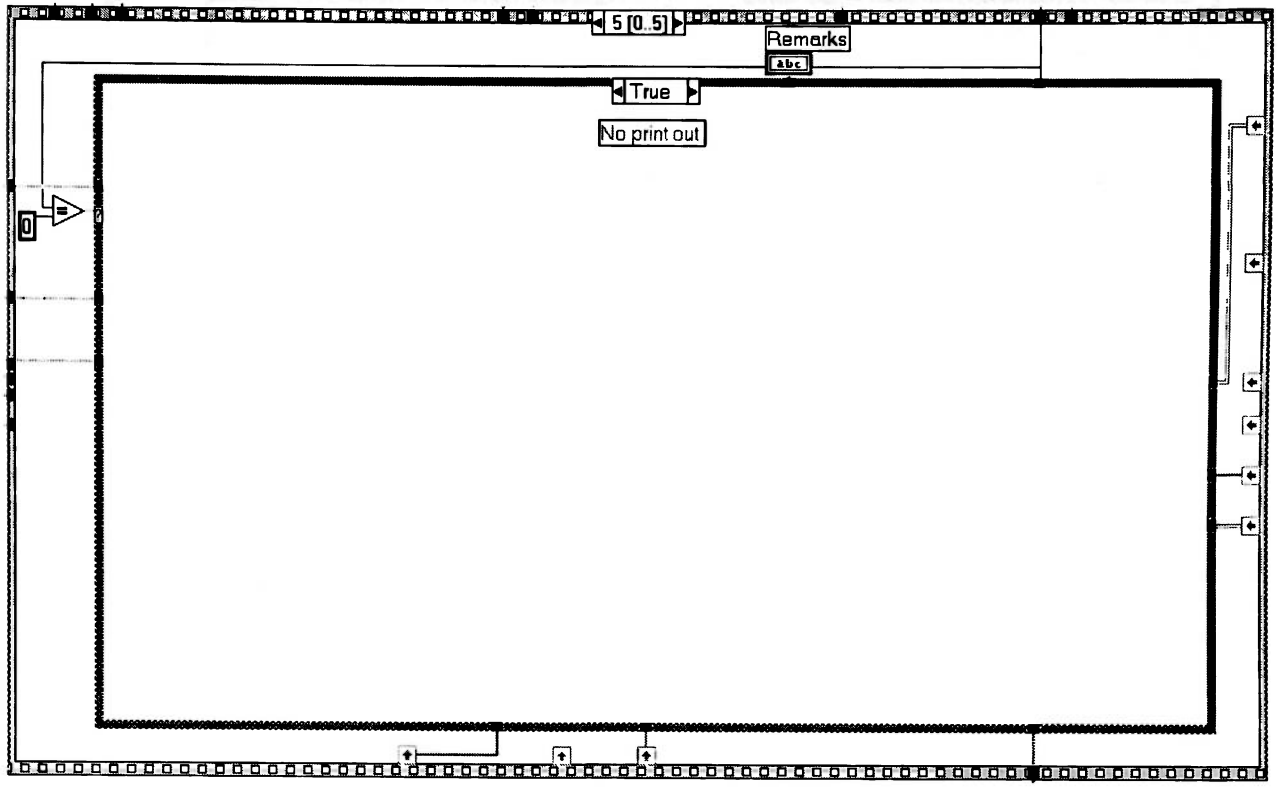

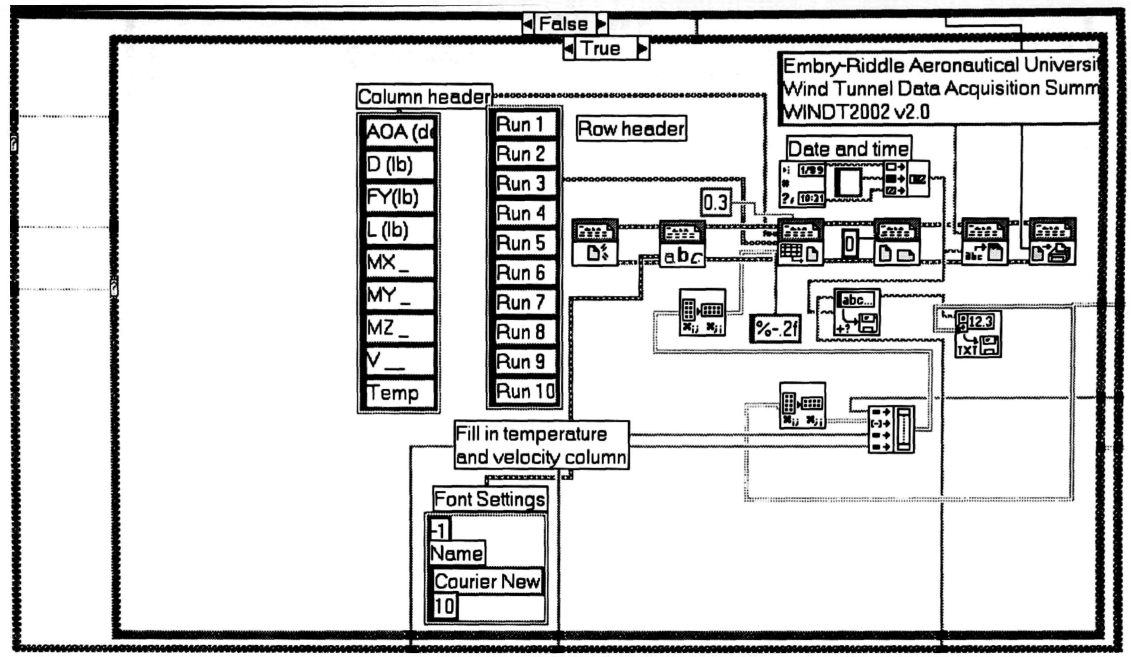
False
True
Column header
AOA (d
D (lb)
FY(lb)
L (lb)
MX_
MY_
MZ_
V__
Temp
Run 1
Run 2
Run 3
Run 4
Run 5
Run 6
Run 7
Run 8
Run 9
Run 10
Row header
Embry-Riddle Aeronautical Universi
Wind Tunnel Data Acquisition Summ
WINDT2002 v2.0
Date and time
0.3
%-.2f
Fill in temperature
and velocity column
Font Settings
-1
Name
Courier New
10

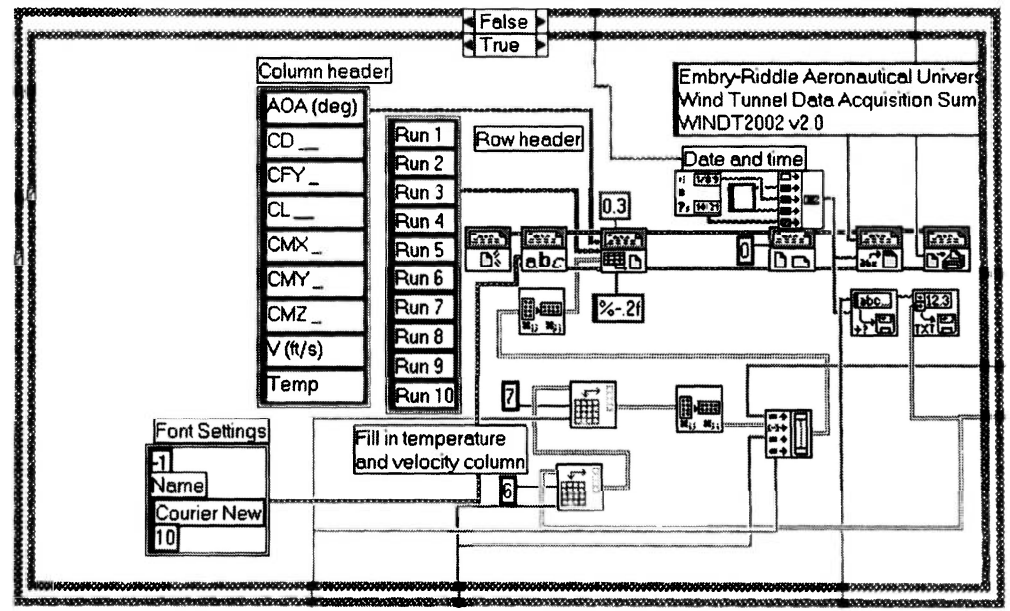
False
True
Column header
AOA (deg)
CD__
CFY_
CL__
CMX_
CMY_
CMZ_
V (ft/s)
Temp
Run 1
Run 2
Run 3
Run 4
Run 5
Run 6
Run 7
Run 8
Run 9
Run 10
Row header
Embry-Riddle Aeronautical Univers
Wind Tunnel Data Acquisition Sum
WINDT2002 v2.0
Date and time
0.3
%-.2f
7
6
Font Settings
-1
Name
Courier New
10
Fill in temperature
and velocity column

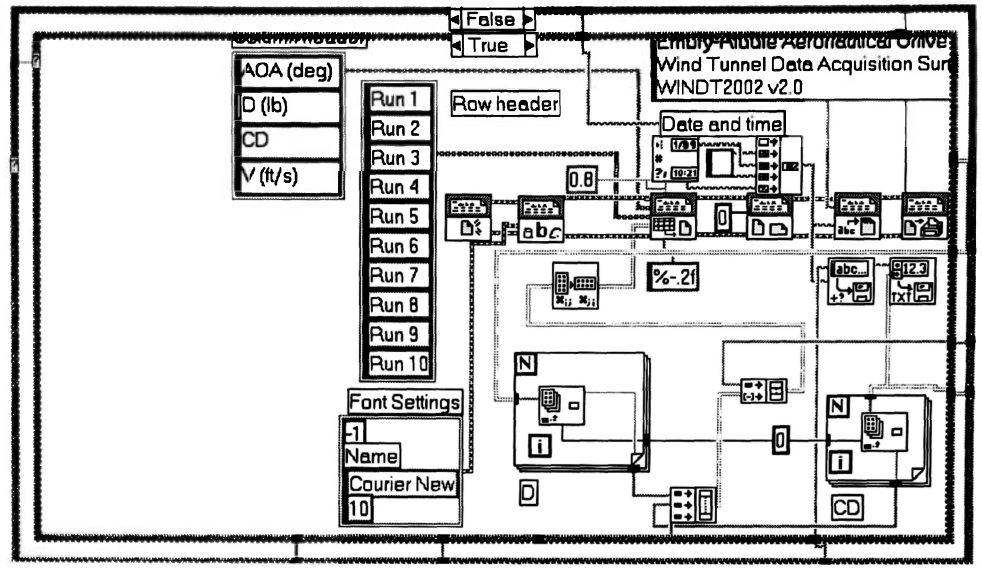
False
True
AOA (deg)
D (lb)
CD
V (ft/s)
Run 1
Run 2
Run 3
Run 4
Run 5
Run 6
Run 7
Run 8
Run 9
Run 10
Row header
Date and time
Wind Tunnel Data Acquisition Sur
WINDT2002 v2.0
0.8
%-.2f
Font Settings
-1
Name
Courier New
10
D
CD

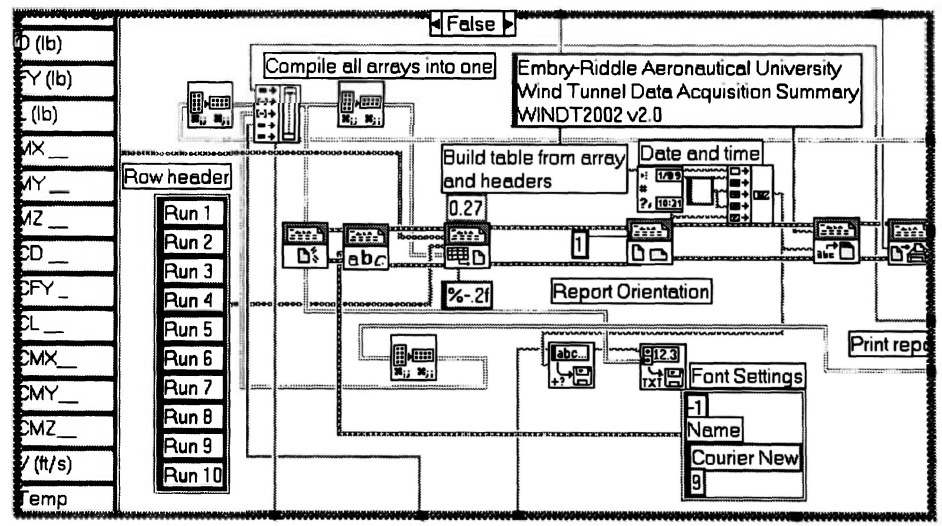
False
Compile all arrays into one
Embry-Riddle Aeronautical University
Wind Tunnel Data Acquisition Summary
WINDT2002 v2.0
Build table from array
and headers
Date and time
Row header
Run 1
Run 2
Run 3
Run 4
Run 5
Run 6
Run 7
Run 8
Run 9
Run 10
0.27
%-.2f
Report Orientation
Font Settings
-1
Name
Courier New
9
Temp

Acq8chan.vi

This sub VI reads voltages from 8 channels at number of scan and rate desired, and returns the averages of the 8 channels.

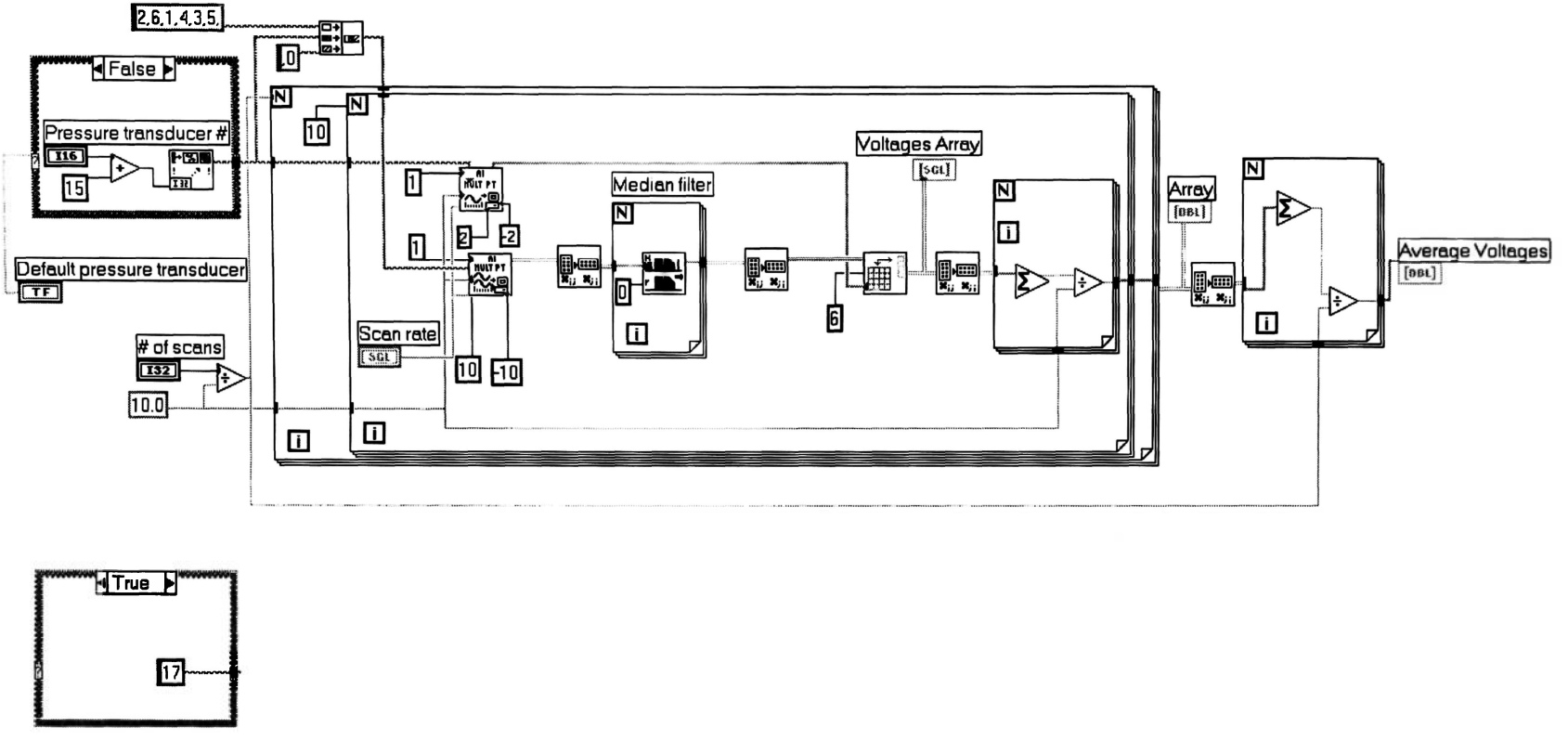

MT.vi

This sub VI peforms moment transfer with given vertical and horizontal moment transfer distances.

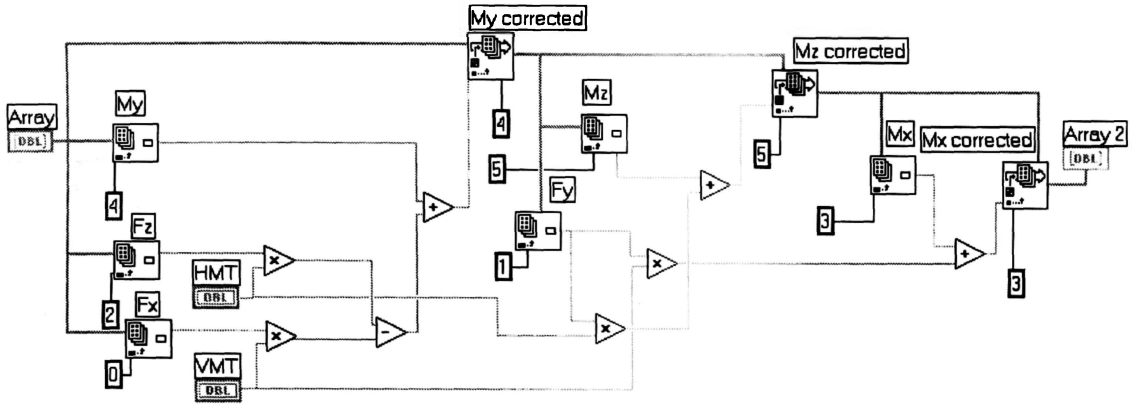

Velocity.vi

This sub VI calculates velocity from an array containing signals from 8 channels.

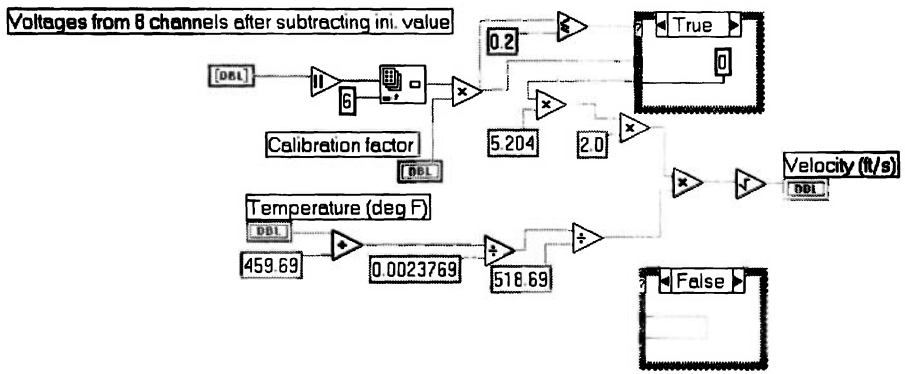

APPENDIX C

PCI-MIO-16E-1, PCI-MIO-16E-4 and NI PCI-6071E Block Diagram (from Ref. 4)

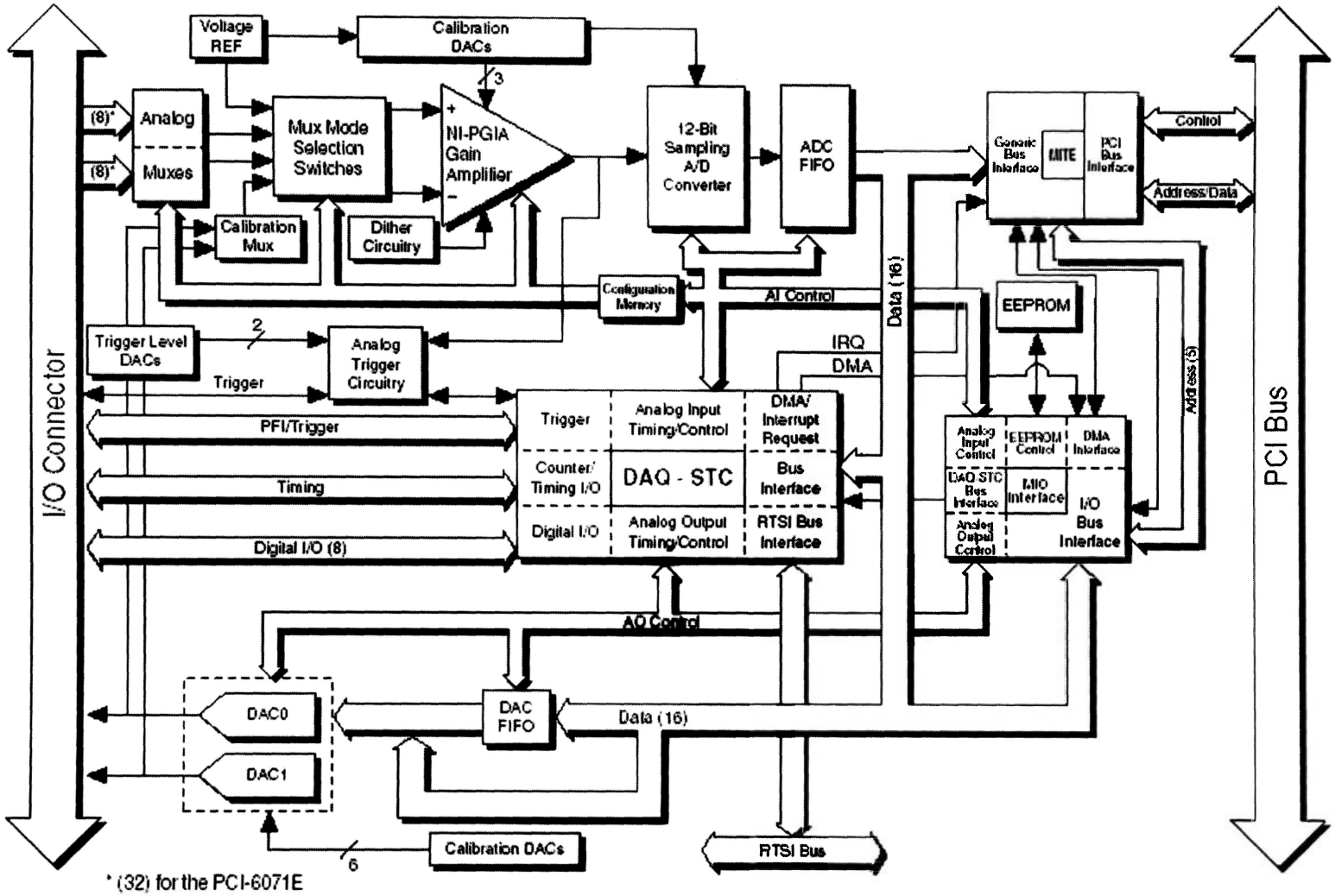

P300D Pressure Transducer Block Diagram (from Ref. 6)

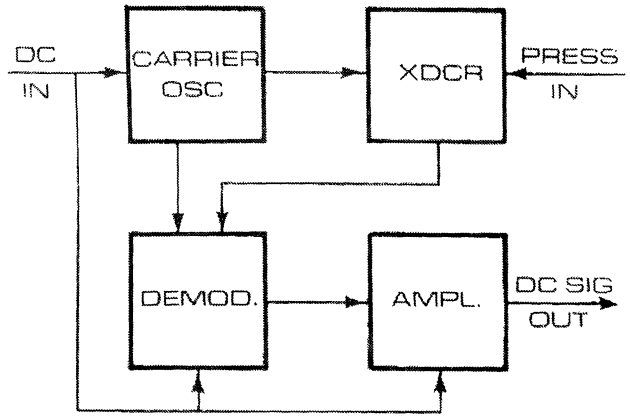

APPENDIX D

Force Balance Pre-Amp System Circuit Diagram (provided by Mike Potash)

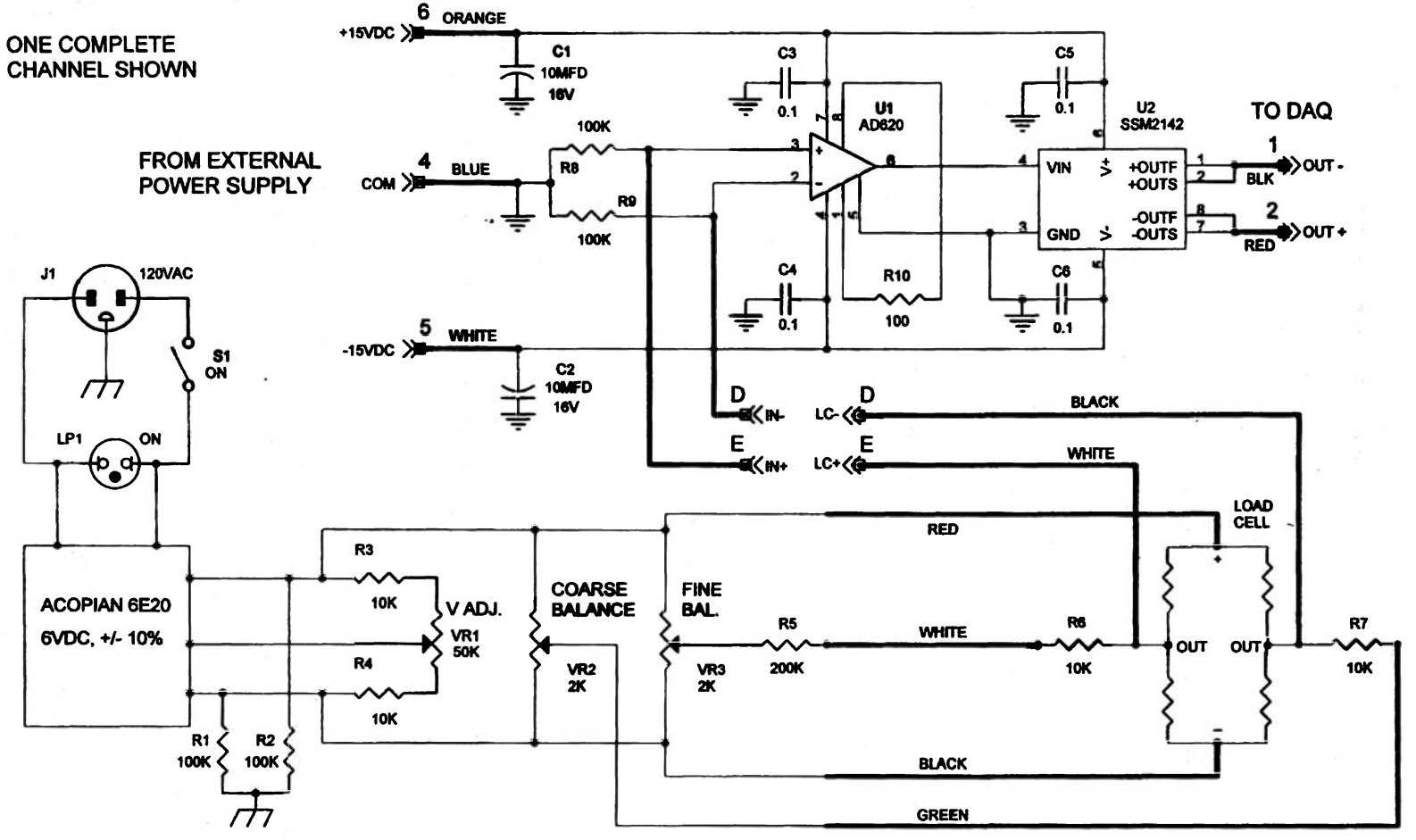

* ALL RESISTORS METAL FILM, 1% *
* HEAVY LINES DENOTE CABLE *
CASE CONNECTION: PIN 3, PIN A

Pressure Transducer Amplifier Circuit Diagram (provided by Mike Potash)